THERMAL PERFORMANCE EVALUATION OF PHASE CHANGE MATERIALS IN BUILDING WALL APPLICATIONS AND COMPARATIVE ANALYSIS WITH INSULATION

A THESIS SUBMITTED TO
GRADUATE SCHOOL OF NATURAL AND APPLIED SCIENCES
OF
KOCAELİ UNIVERSITY

BY
EKREM TUNÇBİLEK

IN PARTIAL FULFILLMENT OF THE REQIREMENTS
FOR
THE DEGREE OF MASTER OF SCIENCE
IN
MECHANICAL ENGINEERING

KOCAELİ 2023

THERMAL PERFORMANCE EVALUATION OF PHASE CHANGE MATERIALS IN BUILDING WALL APPLICATIONS AND COMPARATIVE ANALYSIS WITH INSULATION

A THESIS SUBMITTED TO
GRADUATE SCHOOL OF NATURAL AND APPLIED SCIENCES
OF
KOCAELİ UNIVERSITY

BY
EKREM TUNÇBİLEK

IN PARTIAL FULFILLMENT OF THE REQIREMENTS
FOR
THE DEGREE OF MASTER OF SCIENCE
IN
MECHANICAL ENGINEERING

KOCAELİ 2023

Prof. Dr. Müslüm ARICI **Supervisor, Kocaeli University**	………………………
Prof. Dr. Hasan KARABAY **Jury member, Kocaeli University**	………………………
Associate Prof. Dr. Michal KRAJČÍK **Jury member, Slovak University of Technology**	………………………

Thesis Defense Date: 09.01.2023

ETHICAL STATEMENT AND RESEARCH FUND SUPPORT

In this thesis/project study, which I prepared in accordance with the thesis writing rules of Kocaeli University Graduate School of Natural and Applied Sciences,

I declare that,

- This thesis/project is my own and an original work,
- I act in accordance with scientific ethical principles and rules at all stages of my study, including preparation, data collection, analysis, and presentation of information,
- I have cited all data and information obtained within the scope of this study and that I have included these sources in the bibliography,
- This study complies with the similarity criteria determined by the Graduate School of Natural and Applied Sciences of Kocaeli University in terms of the plagiarism software to which Kocaeli University is subscribed,
- I have not done any falsification of the data used,
- I have not submitted any part of this thesis/project as another thesis/project work at this university or another university.

☒ Any stage of this thesis/project work has not been provided any financial/infrastructural support by any institution/organization.

☐ The data and information produced within the scope of this thesis/project work were carried out by .... with the financial/infrastructure support within the scope of the project no ....

I declare that I accept all the moral and legal consequences at any time that may arise regarding my work in the event of situation contrary to this statement.

....
(Signature)
....
Ekrem TUNÇBİLEK

PUBLISHING AND INTELLECTUAL PROPERTY RIGHTS

[ ] With the decision of the institute board of directors, the opening of my thesis/project to access has been postponed for 2 years from the date of graduation.

[ ] With the reasoned decision of the institute board of directors, the opening of my thesis/project to access has been postponed for 6 months from the date of graduation.

[X] No confidentiality decision has been made regarding my thesis/project.

....
(Signature)
....
Ekrem TUNÇBİLEK

PREFACE AND ACKNOWLEDGEMENTS

I would like to thank my supervisor Prof. Dr. Müslüm ARICI for his consistent support, patience, and valuable guidance throughout this thesis. His expertise and knowledge which he provides generously have helped to strengthen my encouragement within my academic life. I would also like to thank Mechanical Engineering Department staff who in one way or another assisted in the process of my courses and thesis. Last but not least, my deep appreciation goes out to my family for their permanent and invaluable support along with strong trust all through my life.

January – 2023 Ekrem TUNÇBİLEK

CONTENTS

LIST OF FIGURES

LIST OF TABLES

INDEX OF SYMBOLS AND ABBREVIATIONS

α	: Thermal diffusivity, (m^2/s)
Bi	: Biot number
c_p	: Specific heat capacity, (J/(kg·K))
C1	: Case with PCM located near indoor
C2	: Case with PCM located near outdoor
C3	: Case with insulation located near indoor
C4	: Case with insulation located near outside
C5	: Case with PCM is closer to indoor for inside location
C6	: Case with insulation is closer to indoor for inside location
C7	: Case with PCM is closer to outside for outside location
C8	: Case with insulation is closer to outside for outside location
C9	: Case with PCM is located near indoor while insulation is located near outdoor
C10	: Case with Insulation is located near indoor while PCM is located near outdoor
ρ	: Density, (kg/m^3)
Δx	: Step size in spatial coordinates, (m)
Δt	: Step size in temporal coordinates, (s)
E_{LH}	: Energy saving due to latent heat activation, (J/m^2)
E_{PCM}	: Energy saving due to PCM utilization, (J/m^2)
E_{PSM}	: Energy saving due to PSM utilization, (J/m^2)
E_{INS}	: Energy saving due to insulation utilization, (J/m^2)
f	: Liquid fraction
f_D	: Decrement factor
Fo	: Fourier number
h	: Total enthalpy, (J/kg)
h_{out}	: Convective heat transfer coefficient for outdoor, ($W/(m^2 \cdot K)$)
h_{in}	: Convective heat transfer coefficient for indoor, ($W/(m^2 \cdot K)$)
t	: Time, (s)
T	: Temperature, (℃, K)
T_f	: Phase transition temperature, (℃, K)
$T_{f,opt}$	: Optimum phase transition temperature, (℃, K)
T_0	: Surface temperature, (℃, K)
T_i	: Initial temperature, (℃, K)
T_{max}	: Maximum temperature, (℃, K)
T_{min}	: Minimum temperature, (℃, K)
$T_{sol\text{-}air}$	: Solar air temperature, (℃, K)
k	: Thermal conductivity, (W/(m·K))
L_H	: Latent heat capacity, (J/kg)
L	: Total length of the composite wall, (m, mm)
$L_{PCM,opt}$	: Optimum phase change material thickness, (m, mm)
L_{PCM}	: Phase change material layer thickness, (m, mm)
L_{PSM}	: Phase stabilized material layer thickness, (m, mm)
L_{INS}	: Insulation material layer thickness, (m, mm)
ψ	: Phase change material thickness ratio
i	: Modeled node in domain

$i+1$, $i-1$: Neighboring nodes to modeled node
n : Current time step
$n+1$: Next time step
P : One-day period, (s)
ϕ : Time lag, (s)
Q_{PCM} : Energy demand, (J/m^2)
u : An arbitrary function
x_i : Interphase position (m)

Abbreviations

GHG : Greenhouse Gas
GWP : Global Warming Potential
IEA : International Energy Agency
LCC : Life Cycle Cost
LH : Latent Heat
NZE : Net Zero Emissions
PCM : Phase Change Material
PSM : Phase Stabilized Material

FAZ DEĞİŞTİREN MALZEMELERİN BİNA DUVARI UYGULAMALARINDAKİ ISIL PERFORMANSININ DEĞERLENDİRİLMESİ VE YALITIM İLE KARŞILAŞTIRMALI ANALİZİ

ÖZET

Faz değiştiren malzeme (FDM) içeren bir bina duvarının ısıl performans analizi üç farklı yaklaşıma bağlı olarak yapılmıştır. Faz değişim sıcaklığı, FDM kalınlığı ve FDM konumu ısıl analize dayanarak optimize edilmiştir. Seçilen yöntemin FDM'nin enerji tasarrufu üzerindeki etkisini ortaya çıkarmak için her bir yaklaşımda elde edilen optimum değerler verilmiş ve karşılaştırmalı olarak tartışılmıştır. Ayrıca, FDM ve yalıtımın enerji tasarrufu performansları aynı koşullar dikkate alınarak karşılaştırılmıştır. Buna ek olarak, FDM ve yalıtımın kombinasyonu duvarın toplam kalınlığı sabit tutulup karşılaştırılmıştır. Dış ortam sınır koşulu için güneş-hava sıcaklığı yaklaşımı kullanılmıştır. Günlük erime ve katılaşma döngülerinin oluşumunu arttırmak ve böylece gizli ısının maksimum seviyede kullanılabilmesini sağlamak için varsayımsal bir sıcaklık aralığı dikkate alınmıştır. Sonlu fark yaklaşımına dayalı olarak Fortran programlama dilinde bir sayısal kod geliştirilmiştir. Geliştirilen kod sırasıyla Neumann'ın faz değişim çözümü ve deneysel bir çalışmayla analitik ve deneysel olarak doğrulanmıştır. Yöntem-3 ile yapılan ısıl analizlere göre, 8 mm ve 24 mm optimum kalınlık değerleri sırasıyla iç konum ve dış konum için bulunmuş, ancak Yöntem-1 herhangi bir optimum kalınlık değeri sağlamamıştır. Çalışmadaki bulgular, 6 mm kalınlık ve iç konumdaki enerji tasarrufu dikkate alındığında, FDM'nin yalıtıma göre % 16,1 daha iyi performans sağladığını ortaya çıkarmıştır. Ayrıca, duvarda 2 mm FDM ve 38 mm yalıtım kullanılması aynı konumda 40 mm yalıtım kullanılması durumuna göre daha fazla enerji tasarrufu sağlamıştır. Bu şekilde, buna karşılık gelen enerji tasarrufunun 40 mm yalıtım kullanma durumuna göre % 7,3 arttırılabileceği görülmüştür.

Anahtar Kelimeler: Bina Isıl Yönetimi, Enerji Tasarrufu, Faz Değiştiren Malzeme, Gizli Isı, Isıl Performans Değerlendirmesi.

FAZ DEĞİŞTİREN MALZEMELERİN BİNA DUVARI UYGULAMALARINDAKİ ISIL PERFORMANSININ DEĞERLENDİRİLMESİ VE YALITIM İLE KARŞILAŞTIRMALI ANALİZİ

GENİŞLETİLMİŞ ÖZET

Faz değiştiren malzemeler (FDM) son yıllarda birçok alanda kullanılmakta olup bu malzemelerin çeşitli uygulamalarda enerji tasarrufu sağlanması konusunda yüksek bir potansiyeli olduğu literatürde yer alan birçok çalışmada gösterilmiştir. FDM'lerin başlıca kullanım alanları olarak ısıl enerji depolama sistemleri, fotovoltaik panellerin soğutulması, elektronik komponentlerin soğutulması ve bina enerji tasarrufu uygulamaları sayılabilir. FDM'lerin bu tür uygulamalarda tercih edilmesinin başlıca nedeni bu malzemelerin sahip oldukları yüksek gizli ısı kapasiteleridir. Bu malzemeler yüksek gizli ısı kapasiteleri sayesinde yüksek miktarda ısıl enerjiyi daha sonraki bir zaman diliminde kullanılmak üzere depolayabilmektedir. Ayrıca gerekli çalışmaların yapılmasıyla enerjinin depolanma ve kullanım süreçleri optimize edilerek enerjiden elde edilebilecek fayda artırılabilir. Bu tür bir kullanım şekli özellikle güneş ve rüzgar enerjisi gibi kesintili yenilenebilir enerji kaynaklarının daha etkin kullanılmasında önemli rol oynamaktadır. Son yıllarda, FDM'lerin binalarda enerji tasarrufu, sıcaklık dalgalanmalarının azaltılması, termal konfor sağlanması ve bunlara bağlı olarak karbon emisyonlarının azaltılması amacıyla bina cephelerine uygulanması hususunda araştırmalar hız kazanmaktadır. Bu çerçevede, iklim ve çevre şartlarına göre en fazla faydayı sağlayabilecek FDM mühendislik hesapları ile tespit edilerek bina cephesine yerleştirilebilmektedir. Bina cephesine entegre edilen FDM, yaklaşık olarak sabit sıcaklıkta faz değişimi gerçekleştirme ve faz değişim sırasında yüksek miktarda enerji depolama/salma kabiliyetlerine sahip olması sebebiyle iç ve dış ortam arasındaki ısı transferini ciddi derecede kısıtlayabilmekte ve böylece iç ortamın ısıtılması veya soğutulması için gerekli enerjiyi hatırı sayılır ölçüde azaltabilmektedir. Bu noktada en kritik parametre, FDM'nin faz değişim sıcaklığı olmaktadır. Öyle ki, iç ve dış ortam koşullarına uygun faz değişim sıcaklığına sahip bir FDM kullanılmadığı takdirde, söz konusu gizli ısının kullanımı tasarım sıcaklıklarında faz değişimi gerçekleşmeyeceği için neredeyse mümkün olmayacaktır. Gizli ısının kullanılmadığı durumda ise daha önce belirtilen yüksek miktarda enerji soğurulması veya salımı gerçekleşemeyecektir ve FDM kullanımından beklenilen performans alınamayacaktır. FDM'lerin bina cephesinde kullanımında malzemenin duvar içindeki konumu ve kalınlığı da enerji tasarrufunu etkileyen diğer önemli parametrelerdir. Bu kritik noktalar sebebiyle bahsi geçen bu parametrelerin titiz bir mühendislik çalışması ile optimize edilmesi, binalarda FDM kullanımı için son derece önemli hale gelmektedir. Bu noktadan yola çıkılarak bu çalışma kapsamında bina cephelerinde FDM kullanımı durumunda FDM'nin faz değişim sıcaklığı, FDM'nin konumu ve FDM'nin kalınlığının optimize edilmesi amaçlanmıştır. Literatürde FDM içeren bir duvarın ısıl performansının değerlendirilmesi için farklı yaklaşımlar kullanıldığı ancak bu konuda araştırmacılar arasında herhangi bir fikir birliği olmadığı görülmüştür. Bu sebeple tez kapsamında gerçekleştirilen optimizasyon çalışması, seçilen üç farklı metoda göre yapılmış ve bu metotların optimize edilen parametreler ve enerji tasarrufu

üzerindeki etkisi incelenmiştir. Ayrıca ısı transferini azaltmak için geleneksel olarak kullanılan bir yalıtım malzemesi ile FDM'nin ısıl performansları aynı şartlar altında karşılaştırılmıştır. Buna ek olarak FDM ve yalıtımın duvar içerisinde aynı anda kullanılması durumunda sağladıkları ısıl performansı değerlendirmek adına farklı FDM kalınlık oranları dikkate alınarak FDM + yalıtım kombinasyonu için ısıl analizler yapılmıştır. Çalışmada dış ortam sınır koşulu için güneş-hava sıcaklığı yaklaşımı kullanılmıştır ve FDM'nin erime-katılaşma döngülerinin oluşma olasılığını artırmak için varsayımsal bir sıcaklık aralığı seçilmiştir. Sonlu fark yaklaşımına dayalı olarak Fortran programlama dilinde bir kod geliştirilmiştir. Geliştirilen bu kod sırasıyla Neumann'ın faz değişim çözümü ve deneysel bir çalışmayla analitik ve deneysel olarak doğrulanmıştır. Elde edilen sonuçlara göre, optimum faz değişim sıcaklığı Yöntem-1 ve Yöntem-3'e göre kalınlıktan bağımsız olarak iç konum için 22 ℃ bulunmuştur. Ancak Yöntem-2 baz alındığında, bu değerin kalınlığa bağlı olarak 21 ℃ ve 23 ℃ arasında salındığı görülmüştür. Yöntem-1 herhangi bir optimum kalınlık değeri sunmazken Yöntem-2 dış konum için 34 mm optimum kalınlık değeri önermiştir. Ancak Yöntem-3 hem iç konum hem de dış konum için birer optimum yalıtım kalınlığı değerini işaret etmiş olup bu değerler sırasıyla 8 mm ve 24 mm olarak bulunmuştur. Çalışmadaki bulgulara göre, iç konum dikkate alındığında 6 mm FDM kullanılması durumu aynı konumda 6 mm yalıtım kullanılması durumuna göre % 16,1 daha fazla enerji tasarrufu sağlamıştır. Ayrıca duvar içerisinde FDM ve yalıtım kombinasyonu kullanılması durumunda, 2 mm FDM ve 38 mm yalıtım kullanılması durumu aynı konumda 40 mm yalıtım kullanılması durumuna göre daha fazla enerji tasarrufu sağlamış ve bu tasarruf oranının duvar konfigürasyonuna bağlı olarak % 7,3'e kadar çıkabileceği görülmüştür.

THERMAL PERFORMANCE EVALUATION OF PHASE CHANGE MATERIALS IN BUILDING WALL APPLICATIONS AND COMPARATIVE ANALYSIS WITH INSULATION

ABSTRACT

Thermal performance evaluation of phase change material (PCM) integrated building wall is conducted based on three different approaches. Optimization of PCM melting temperature, thickness, and location is performed based on thermal analysis. Obtained optimal values depending on each approach is given and discussed comparatively to reveal the effect of chosen method on energy saving performance of PCM. Besides, energy saving performance of PCM and insulation is compared by considering the same conditions. Moreover, combination of PCM and insulation is studied while the total thickness of the wall is kept constant. The solar-air temperature is employed for the outdoor boundary conditions. A hypothetical temperature range is considered in order to increase the occurrence of daily melting and solidification cycles so exploitation of latent heat can be maximized. An in-house numerical code is developed in Fortran programming language based on the finite difference approximation. The code is validated analytically and experimentally by Neumann's solution of phase change and an experimental work, respectively. Based on the thermal analyses with Method-3, 8 mm and 24 mm PCM optimum thicknesses are found for inside and outside locations, respectively, while Method-1 provides no optimum thickness value. The findings revealed that PCM outperforms insulation by 16.1 % in terms of energy saving at 6 mm thickness for inside location. In addition, using 2 mm PCM and 38 mm insulation material in the wall saves more energy than using 40 mm insulation at the same location. In this case, the corresponding energy saving can be increased by up to 7.3 % compared to 40 mm insulation.

Keywords: Building Thermal Management, Energy Saving, Phase Change Material, Latent Heat, Thermal Performance Evaluation.

1. INTRODUCTION

Energy demand continues to rise globally driven by rapid population growth, improved access to energy services, and urgent energy need in developing countries. Since the energy production is still highly dependent on non-renewable energy sources such as coal, natural gas, and oil, there is a widespread concern among experts that the energy supply chain may not be sustained properly in the future (International Energy Agency, 2021a). Therefore, transition to renewable energy sources and reduction of energy demand are crucial to provide energy security. Furthermore, it is a known fact that the current energy production causes a significant amount of greenhouse gas (GHG) emissions to the atmosphere. Considering the global energy sector is accounted for about three-quarters of the GHG emissions that have caused visible extreme weather and climate events especially in the recent years, it is obvious that actions related to the mitigation of climate change have to be initiated from the energy sector (International Energy Agency, 2021c). As the literature pointed out, in order to avoid the approaching severe consequences of climate change in the upcoming years and maintain a livable environment, global average temperature rise has to be limited to 1.5 °C (until 2050) compared to the pre-industrial era. It is clear that emergent actions have to be taken considering the global average temperature has already been pushed by 1.1 °C. Therefore, according to the Paris Agreement, the Net Zero Emission (NZE) target has been put aiming to completely diminish the GHG emissions by 2050 (International Energy Agency, 2021b). In order to reach to the predetermined targets in the way to clean energy and emission-free society, the current energy demand as well as the increasing trend has to be commanded. The International Energy Agency (IEA) encourages energy-related sustainable development goals such as electrification of vehicles, enhancement of efficiency of household appliances, adaptation of building codes for built environment, and integration of renewable energy sources to energy grid (International Energy Agency, 2021b, 2021c). In this context, an urgent economic and social transformation plan driven by a strong desire for clean energy and environment has to be initiated immediately.

Buildings have a major role in people's daily lives and therefore in the society since they form and frame the environment that people interact within, live, and work. In the transition to a sustainable and resilient society induced with clean energy, buildings can be a significant part of the process due to their primary impact on the GHG emissions and energy consumption. According to the report prepared by United Nations Environment Programme (UNEP) (United Nations Environment Programme, 2021), the buildings and construction sector account for about 36 % of the global final energy demand. Along with that, the share of the buildings and construction sector in the energy-related CO_2 emissions is 37 % taking into account both direct as well as indirect emissions. Considering that most of the countries still lack proper policies and codes for built environment, new buildings that will be constructed in the upcoming years will be no-question the source of the future GHG emissions and energy demand increase. Especially when the growing population and urbanization in the rapid developing countries is considered, the floor area is expected to be doubled by 2050. However, the existing building stock will still represent a major part of the floor area meaning that retrofitting buildings will be also crucial (Z. Zhou et al., 2016). Therefore, it can be stated that implementing mandatory building energy codes, developing decarbonization strategies for retrofitting/refurbishment, increasing efficiency of appliances, and promoting clean energy are the main solutions for achieving the NZE targets (Global Alliance for Buildings and Construction et al., 2020).

According to the application purpose, transparent or non-transparent components are utilized in building external envelopes, and windows and walls can respectively be considered as examples of such components in buildings. As expected, each building envelope type pose specific challenges related to its own material structure and different effects are observed on the energy performance (Long & Ye, 2015). The design of building envelopes is of great importance since they determine the heating and cooling energy requirement, provide thermal comfort, maintain indoor environment quality, and preserve the inhabitants from surrounding climatic conditions exposure. Therefore, the selection of building external envelope composition and material is significant considering the long lifetime of buildings and the related costs. As mentioned earlier, most of the countries still lack proper building envelope standards meaning buildings located in these countries cause excessive energy demand. Besides, even in the countries which adopt energy-efficient building codes, there is an existing-stock problem waiting to be resolved by retrofitting. For the time being, these are the main challenges related to building sector need rapid solutions so the NZE targets can be reached, and a sustainable as well as a green future can be secured. In this regard, energy performance of buildings can be enhanced by installing insulation material in building external envelope (roof, wall, and floor) (Dombaycı et al., 2006; Kaynakli, 2012), increasing thermal mass of the building (Baetens et al., 2010; D. Li et al., 2022), optimizing building orientation (Morrissey et al., 2011), preventing thermal bridges in the envelope structure (Martin et al., 2011; Theodosiou & Papadopoulos, 2008), and using glazing with high thermal performance (Buratti et al., 2021; Cuce & Riffat, 2015).

One of the most obvious solutions to reduce energy demand and thus the environmental impact is the utilization of insulation material in the building external envelope (Papadopoulos, 2005). Thermal insulation materials are known for their extremely low thermal conductivity, so they are able to reduce the heat transfer between the indoor and outdoor environments by increasing the thermal resistance in the external wall significantly. For instance, Çomaklı and Yüksel (Çomakli & Yüksel, 2003) investigated the effect of using insulation material in the external walls of the buildings located in the coldest cities of Türkiye. The life cycle cost (LCC) analysis was employed to optimize the insulation layer thickness. According to the findings of the study, the authors stated that a great amount of energy can be saved, and the payback period varied between 1.40 years and 1.51 years meaning that the costs were covered under two years of operation after the installation of insulation. The same authors conducted another study (Çomakli & Yüksel, 2004) focusing on the environmental effects of using insulation in building external walls and found that 27% reduction in CO_2 emissions can be achieved by applying optimum insulation thickness. An economic and environmental analysis of integrating insulation into building wall was carried out by Dombaycı (Dombayci, 2007). It was stated that up to 46.6% decrease in the energy consumption and 41.5% decrease in the GHG emissions can be accomplished by using optimum insulation thickness. A comprehensive study focusing on the determination of optimum insulation thickness for building external walls was carried out by Bolattürk (Bolattürk, 2006) considering five different heating fuel sources based on the LCC analysis. In order to compute the results, 16 different cities were chosen from four different climatic zones of Türkiye. The obtained findings revealed that the used fuel source for heating affected the optimum insulation thickness and payback period. Besides, it was stated that the energy saving rate can reach up to 79 % while payback periods were calculated between 1.3 years and 4.5 years depending on the considered city as well as the fuel source which coal and natural gas was found to be most appropriate choices. Yu et al. (Yu et al., 2009) carried out a study concerning the effect of insulation integration on the payback period and savings. In the study, hot summer and cold winter zone of China was considered for thermal analyses, and different climatic conditions in this zone were evaluated. According to the obtained results, a great amount of was energy saved, and the optimum insulation thicknesses varied from 5.3 cm to 23.6 cm while the payback periods were between 1.9 years and 4.7 years. A study conducted by Özel (Ozel, 2011) focused on the potential impact of building wall orientation on determining optimum insulation thickness. Based on the findings presented, it was revealed that the wall orientation differed the optimum insulation thickness, and the south orienting wall had a lower insulation thickness than the other orientations of walls. Reportedly, the wall orientations other than the south orientation needed 0.5 cm thicker insulation layer under the considered climatic conditions. It was also reported that the highest energy saving was attained on the north orienting wall whereas the lowest energy saving was acquired with the south orienting wall. Energy saving amount can reach 51.2 $/m^2 with a 1.36 years of payback period. Tunçbilek et al. (Tunçbilek et al., 2022) investigated the effect of operation schedule of the building on the optimum insulation thickness, and thus energy saving as well as global warming potential (GWP). In the study, two different intermittently operated building types (House and Office) were considered, and the obtained results were evaluated. The results showed that the operation type of the building had a major impact on the optimum insulation thickness. According to the findings given, energy demand was reduced approximately by 63 % and 74 % for the case of House and Office, respectively. In addition to that, a reduction of up to 62 % for the total GWP index was calculated for the House operated building. In another study, Huang et al. (Huang et al., 2020) investigated the potential effects of using aerogel in the external wall of an typical office building on the energy saving as well as the GHG emissions. It was reported that 18 % reduction in yearly heat load can be achieved. Besides, the thermal insulation with optimum insulation thickness enabled to prevent roughly 8.2 kg/(m^{2}year) GHG emissions when natural gas was chosen as fuel source. Despite the fact that the building energy codes are still not adopted by a majority of countries especially for the developing countries, it is clear that thermal insulation is of great importance to reduce energy consumption and thus related GHG emission for building sector. In this regard, it is important for policy makers, managers, and researchers to inform and encourage end-users for adopting such easy yet effective solution to energy and climate crisis.

Phase change materials (PCMs) are also investigated both from experimental and mathematical aspect in buildings to reduce energy consumption as well as carbon footprint of building sector lately (Hassan et al., 2022; Kuznik et al., 2011). They are categorized according to their chemical structure as organic, inorganic and eutectic, and each type has its own merits and demerits making them desirable depending on the application area (Cabeza et al., 2011). Although PCMs generally have high thermal conductivity compared to insulation materials, their high phase change enthalpy, i.e., latent heat capacity, makes them potentially strong candidates for energy demand reduction in buildings. In addition to that, especially some types of PCMs offer a relatively narrow range for phase change temperature and a phase change temperature close to comfort conditions which can be very useful in indoor thermal environment conditioning. There are many studies in the literature on the application of PCM in buildings, and they vary depending on the application type such as photovoltaic (PV) panels (Kouravand et al., 2022), thermal energy storage tanks (Cao et al., 2022), floor (Cesari et al., 2022), roof (Bhamare et al., 2020), walls (C. Li et al., 2022), glazing (S. Zhang et al., 2022), and sunspaces (Uludaş et al., 2022). Most of these studies concerned PCM integration in building external walls where significant energy saving as well as indoor temperature fluctuation reduction were observed (Lamrani et al., 2021). For instance, Salihi et al. (Salihi et al., 2022) carried out a numerical study to investigate the potential energy saving effect of PCM integrated wall under semi-arid climatic conditions of Morocco. According to the findings of the study, the PCM integration to walls of the building improved the indoor thermal comfort by reducing the indoor temperature fluctuations and saved a significant amount of energy. Furthermore, employing two or three layers of PCM in the walls was found to be more effective in terms of energy saving, and the energy saving rate starting from 7.3 % and reaching up to 15.2 % was achieved by PCM integration. The influence of PCM integrated wall on energy saving was evaluated, and the optimum location for PCM layer was investigated by Sun et al. (Sun et al., 2022). Different parameters like insulation level, phase change temperature, PCM layer thickness was considered in the study. The results showed that up to 50 % reduction in heat flux can be attained by utilizing optimized PCM in the wall. Besides, 7 mm thickness was found to be optimum for PCM layer thickness while a range of 27 ℃ to 31 ℃ phase change temperature gave the best thermal results. Additional insulation thickness shifted the optimum location of PCM towards to the outdoor environment, reportedly. Another research investigating the impact of PCM integration in building external wall on the energy demand reduction was performed by Li et al. (Q. Li et al., 2022). They considered buildings located in 5 different climatic regions of China and evaluated the economic aspects of utilization of PCM also. The study showed that the PCM integration saved around 37 % of energy in Kunming while an energy saving rate around 16 % was observed in Shenzhen. The optimum phase change temperature was generally close to the yearly average temperature of the region where the building located. Based on the economic evaluation, the utilization of PCM in the wall of a building was justified in Harbin giving nearly 6 years of payback time. In a similar study conducted by Souayfane et al. (Souayfane et al., 2019), thermal performance of PCM integration was evaluated along with economic aspect. The PCM was utilized with transparent insulation material (TIM) to be used in the application of a translucent super-insulated PCM wall. The findings suggested the utilization of TIM-PCM wall in polar and subarctic climates since relatively low payback periods were determined (7.8 years to 10.5 years). A comprehensive research was carried out by Kishore et al. (Kishore et al., 2021) considering different parameters affecting the PCM thermal performance integrated in building external wall. The authors reported that locating the PCM layer near the indoor environment can reduce the heat gain up 75 % during the peak periods without increasing the total daily heat gain. Besides, increasing the PCM thickness further over a certain value decreased the heat gain during the peak hours whereas also increased the total daily heat gain. According to the performed sensitivity analysis, the specific heat and thermal conductivity were found to be insignificant while phase change temperature, location, and thickness of PCM was determined as crucial parameters affecting the thermal modulation. Li et al. (S. Li et al., 2019) evaluated the thermal impact of PCM Trombe wall on the thermal comfort and energy loads, and the obtained results were compared with those of a conventional Trombe wall. According to the findings presented, the Trombe wall integrated with PCM decreased the overheating of indoor environment in summer while reduced the indoor temperature fluctuations in winter season. Hamidi et al. (Hamidi et al., 2021) carried out a study concerning the PCM filled hollow brick thermal performance and found that 56 % reduction in energy demand of the building can be achieved depending on the region. A similar study considering PCM filled hollow bricks in the building wall found that PCM integration can cause adverse effects and increase the cooling load during summer season in the case of appropriate selection of phase change temperature (Tunçbilek, Arıcı, Bouadila, et al., 2020). The authors reported that with the optimized PCM filled hollow bricks, 17.3 % reduction in energy demand was obtained compared to reference wall and the contribution of laten heat exploitation on energy saving was significant. In addition to that, locating PCM near the indoor environment performed better than locating it near the outdoor environment, and increasing the PCM amount in the hollow bricks increased the energy saving. In another study Wang et al. (Wang et al., 2016) experimentally investigated the thermal performance of PCM in the external wall a full-scale room. The findings reveal that up to 30 % reduction in heating load and 24.3 % reduction in cooling load can be achieved. Besides, the PCM-wall decreased the peak temperature of interior surface by 0.2 ℃ while increasing the time lag 1 to 2 hours. The influence of PCM integration in external building envelope on the energy saving performance of wall was investigated during winter season (Abu-Hamdeh et al., 2021). The study results showed that energy saving ranging from 10.4 % to 11.3 % can be achieved depending on the month. The economic aspect of installing PCM into the wall was also evaluated, however, the obtained results suggest that PCM installation was no feasible under the considered conditions. Kalbasi et al. (Kalbasi & Afrand, 2022) conducted a study focusing on different thickness ratios for PCM and insulation combination and found that PCM + insulation combination behaved better than only insulation under some certain conditions. Overall, PCM seems to be a promising solution to the energy demand increase of building sector in the upcoming years.

It is clear from the literature review that PCM integration to the external wall of buildings is a great candidate for energy conservation, and thus reduction of CO_2 emissions in the built environment. However, there is still no consensus regarding the measurement of effectiveness of PCM integrated building walls with respect to those of without PCM integration. In contrary to insulation materials, PCMs have different parameters such as phase transition temperature and phase change enthalpy affecting their thermal performance along with thermal conductivity. Therefore, a critical review and a case study of this topic appears as a research gap in the literature that must be filled with deep understanding of the phase change phenomenon as well as energy saving performance of PCM. Apparently, the evaluation of PCM effectiveness in building applications varies depending on the application type. For instance, thermal energy storage/release time and amount are important parameters determining the effectiveness in latent heat thermal energy storage (LHTES) systems for PCMs (Ben Khedher et al., 2022). In building envelope applications on the other hand, the effectiveness of PCM integration can be seen through different parameters. In order to exemplify such parameters, energy consumption, indoor temperature fluctuation, time lag, decrement factor, and load shifting can be enumerated from a very broad perspective. However, Zhang et al. (Y. Zhang et al., 2008) carried out a study focusing on the thermal performance evaluation for PCM wallboards, and stated that the effectiveness of PCM cannot be evaluated by using time lag and decrement factor since the behavior of PCMs highly deviates from other building materials, e.g., insulation material. Therefore, two novel parameters namely modifying factor for the interior surface heat flux and the thermal energy storage ratio were proposed. In another study, three novel different objective functions were put forward by Arnault et al. (Arnault et al., 2010) to evaluate PCM-floor thermal performance. These functions mainly considered heat load curve behavior of PCM integrated floor compared to that of without PCM integration. Shape-stabilized PCM wallboard thermal performance was evaluated through parameters such as time lag, decrement factor, and phase transition keeping time by Zhou et al. (G. Zhou et al., 2010, 2011). A new parameter named Phase Stabilized Material (PSM) was defined by Izquierdo-Barrientos et al. (Izquierdo-Barrientos et al., 2012) regarding the PCM integration. This material actually has the same thermophysical properties with the chosen PCM, however, it does not undergo phase change meaning that there is no latent heat storage or release. Thereby, the PSM containing wall has the same thermal resistance and sensible heat storage/release capacity with that of PCM containing wall enabling to reveal the importance of latent heat exploitation when compared. Another study was conducted by Zwanzig et al. (Zwanzig et al., 2013) which the thermal performance of PCM implementation to building wall was evaluated by peak load shifting/reduction, and yearly heating/cooling energy demand reduction. Sun et al. (Sun et al., 2014) conducted a study concerning the implementation of PCM wallboard to buildings and evaluated the PCM thermal performance through parameters named simple payback period and energy saving ratio (ESR) of air-conditioning (A/C) system. The ESR was basically defined as the ratio of energy consumption of A/C system with PCM wallboard to energy consumption of A/C system without PCM wallboard. A full-size experimental thermal performance evaluation of PCM integration was carried out by Ye et al. (Ye et al., 2014). They proposed a new parameter called energy saving index (ESI) and defined it as the ratio of a building material/component to the ideal thermal performance of that material (also defined as energy saving equivalent). A comprehensive analysis of PCM dynamic behavior was performed by Mazzeo et al. (Mazzeo et al., 2017) and new different set of parameters were introduced to evaluate the PCM thermal performance under non-sinusoidal outdoor temperature fluctuation. The proposed dynamic parameters included the latent heat energy storage efficiency, decrement factor, time lag, and constant peak time fraction. These parameters were used in a case study and reported that the best PCM was chosen among other candidates. Particularly the energy storage efficiency of latent heat is an important parameter since it also considers the primary parameter of using PCM in the first hand, i.e., latent heat storage/release. Indoor air temperature fluctuations, thermal load levelling, and interior surface temperature were employed to evaluate the thermal performance of PCM in another study (Meng et al., 2017). A novel thermal performance indicator named measure of key response index (MKR) was developed by Bhamare et al. (Bhamare et al., 2021). This index was consisted of several parameters such as time lag, decrement factor, and heat gain. A proper selection of PCM then was carried out by the authors based on the MKR index.

The presented literature review proves that both insulation and PCM integration to building external envelopes promise to be powerful tools for energy demand reduction for built environment. Furthermore, it is also obvious that there is no consensus regarding the thermal performance evaluation of PCM integrated building external walls since variety of different parameters are considered in the literature. Therefore, this study focuses on the thermal performance evaluation of PCM in the building external walls by considering three methods/approaches. The study presents a problem which is an optimization study for significant PCM parameters such as the phase change temperature, PCM location, and PCM amount (i.e., through PCM thickness). These parameters are optimized by pre-determined/defined three methods and the obtained optimum values are discussed. Furthermore, the study then reveals the impact of PCM on the energy saving compared to insulation material. It is obvious that head-to-head comparison of PCM and insulation would not be fair since their thermophysical properties and application purposes are rather different, however, the results are still given comparatively to highlight the significant impact of PCM integration on energy saving. Subsequently, the combination of PCM and insulation material is studied by considering different PCM thickness ratios while the total thickness of the wall is kept constant. Consequently, the study provides a comprehensive analysis on the thermal performance evaluation of PCM integrated building external walls, and on the PCM-insulation relations in terms of thermal performance.

2. MATERIALS AND METHOD

In this section of the study, problem definition, mathematical modelling of the problem, discretization of the governing equations, and validation of the developed numerical code is given. Then, PCM performance evaluation methods and their corresponding definitions are given along with related formulas.

2.1. Problem Description

A representative room is considered for the problem to conduct thermal analyses of different evaluation methods/approaches and PCM + insulation performance regarding the PCM integrated building external wall. Heat transfer occurs only through the south-facing wall since the remaining walls are adjacent to the other rooms, i.e., they can be taken as adiabatic. The reference specimen wall is composite and consisted of three layers, namely, inner plaster (10 mm), concrete block (240 mm) and outer plaster (10 mm) from inside to outside environment, respectively (Figure 2.1).

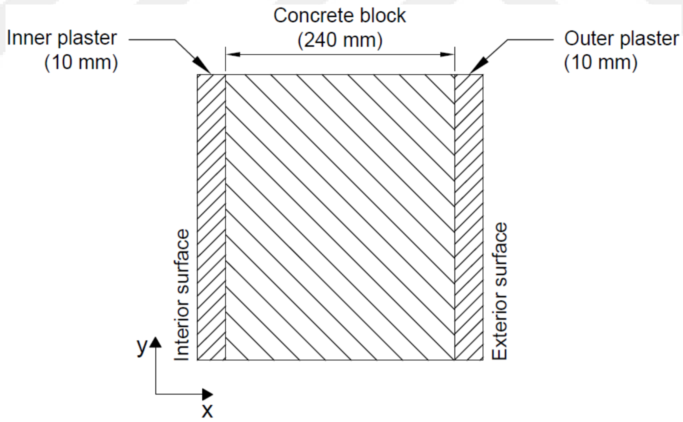

Figure 2.1. The schematic representation of the reference wall (not to scale)

Table 2.1. Thermophysical properties of the composite wall materials

Material	k (W/(m·K))	ρ (kg/m^3)	c_p (J/(kg·K))	L_H (J/kg)	T_f (°C)
Plaster	0.57	1100	1000	–	–
Concrete block	1.41	2100	1000	–	–
Glass wool	0.038	32	840	–	–
PCM	0.2	760 (*l*), 880 (*s*)	2000	134×10^3	Design parameter

The corresponding thermophysical properties of the composite wall materials are given in Table 2.1. An additional PCM layer (L_{PCM}) is added to the reference wall in the case of PCM integrated wall. The location of the extra PCM layer is varied during the simulations to find the best position in the wall for the highest thermal performance. Therefore, the PCM layer is located either between the inner plaster and concrete block (C1) or between the concrete block and outer plaster (C2) (Figure 2.2).

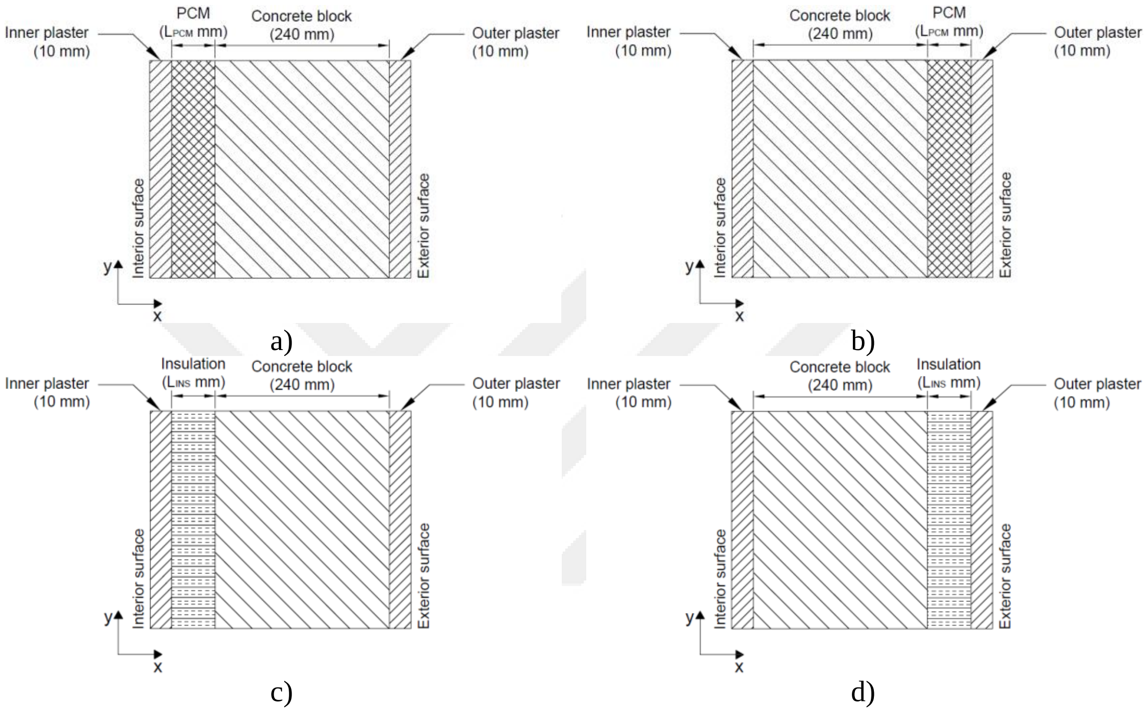

Figure 2.2. The schematic representation of PCM or insulation containing wall. a) PCM located near the indoor (C1), b) PCM located near the outdoor (C2), c) Insulation located near the indoor (C3), d) Insulation located near the outdoor (C4)

Furthermore, different PCM layer thicknesses should be tested in order to reveal the optimum PCM layer thickness if such a value exists. For this purpose, 20 different PCM layer thicknesses ranging between L_{PCM} = 2 – 40 mm (by 2 mm increment) are used in the thermal analyses. Similar to the location as well as thickness of the PCM layer, an optimum case for phase change temperature should also be determined, therefore, 16 various phase change temperatures (T_f = 15 – 30 °C by 1 °C increment) are examined to find the melting temperature giving the highest possible thermal performance. Other thermophysical properties, namely, the density, specific heat, thermal conductivity, and latent heat capacity are taken as constant and given as in Table 2.1. The thermal performance of the considered composite wall is also evaluated with an insulation material, i.e., glass wool is chosen as thermal insulator (Table 2.1). Similar to PCM, different layer thicknesses (L_{INS} = 2 – 40 mm by 2 mm increment) are employed to assess the energy saving amount with respect to reference case. Glass wool is also positioned either between the inner plaster and concrete block (C3) or outer plaster and concrete block (C4) (Figure 2.2). The combined effect of using PCM and insulation material at the same time is also studied. It is evaluated by varying the thickness of PCM and insulation material while the total thickness of the wall is kept constant. In this case, the sum of the total thickness of PCM (L_{PCM}) and insulation material (L_{INS}) is considered as 40 mm (L_{PCM} + L_{INS} = 40 mm). For instance, when L_{PCM} thickness is employed for PCM, that means L_{INS} = 40 – L_{PCM} mm insulation material, i.e., glass wool, is employed. Furthermore, a parameter called thickness ratio (ψ) is defined in Equation (2.1). The given ratio equals to unity when the whole layer is consisted of PCM (ψ = 1) while equals to zero when the whole layer is consisted of insulation material, i.e., glass wool (ψ = 0). The intermediate values for thickness ratio ($0 < \psi < 1$) depicts the layer is consisted of both insulation material (L_{INS}) and PCM (L_{PCM}). For instance, ψ = 0.5 means that 20 mm of PCM (L_{PCM} = 20 mm) and 20 mm of insulation material (L_{INS} = 20 mm) is employed.

$$\psi = \frac{L_{PCM}}{L_{INS} + L_{PCM}} \tag{2.1}$$

The wall configurations for different combinations of PCM and insulation layer is given in Figure 2.3. Both PCM and insulation material locations are varied to investigate the effect of different positions on the thermal performance also. In the given figure, six different configurations of the wall are presented considering that the total length of the wall is kept constant. It should be noted that for each considered location of PCM and insulation material, different thickness ratios of PCM (ranging between 0 and 1) are tested and the thermal performance of the wall evaluated accordingly.

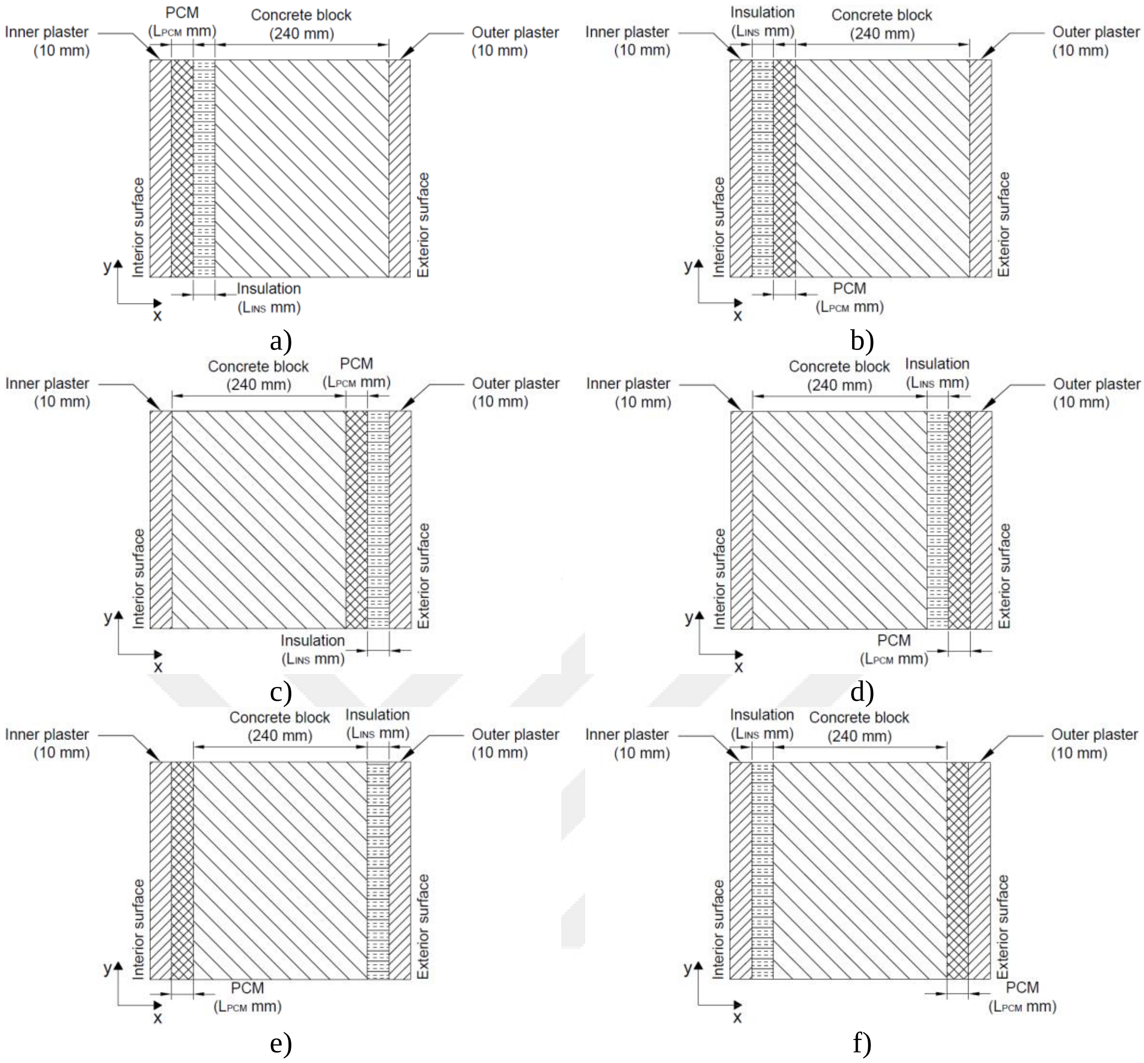

Figure 2.3. The schematic representation of PCM and insulation layer in combination. a) PCM is closer to indoor for inside location (C5), b) Insulation is closer to indoor for inside location (C6), c) Insulation is closer to outdoor for outside location (C7), d) PCM is closer to outdoor for outside location (C8), e) PCM is near indoor, and insulation is near outdoor (C9), f) Insulation is near indoor, and PCM is near outdoor (C10)

2.2. Mathematical Modelling

The heat transfer through the building external wall occurs by pure conduction and can be modelled as one-dimensional in the *x*-direction. The differential equation representing the one-dimensional energy equation in the wall elements except for the PCM is given in Equation (2.2):

$$\rho c_p \frac{\partial T}{\partial t} = \frac{\partial}{\partial x}\left(k \frac{\partial T}{\partial x}\right) \tag{2.2}$$

where, the material properties ρ, c_p, and k represent the density, specific heat capacity and thermal conductivity, respectively. The time-dependent temperature is denoted by T. The spatial coordinate is denoted by x whereas the temporal coordinate is represented by t in the equation. Since the thermal conductivities of the composite wall materials are constant throughout the simulations except for PCM, Equation 2.2 is rewritten by using the derivative at the right-hand side of the equation (Equation (2.3)).

$$\rho c_p \frac{\partial T}{\partial t} = k \frac{\partial^2 T}{\partial x^2} \tag{2.3}$$

The major challenge in modelling of melting and solidification phenomena appearing in PCM problems is the determination of moving interface. This interface separates the solid and liquid phase regions from each other and must satisfy a certain condition called Stefan condition (Jiji, 2000). Because of the non-linearity of the solution for the resulting equation, there are few analytical solutions to the problem which can be used in very limited conditions. Therefore, approximate numerical solutions are employed to obtain solution to these kinds of problems (Özışık, 1980). The numerical procedures applied to these problems can be categorized under three main groups namely, fixed grid methods, deforming grid methods, and hybrid methods. There are different pros and cons regarding each method group, however, the fixed grid methods have been widely preferred in the literature (AL-Saadi & Zhai, 2013). These methods include the enthalpy, heat capacity, temperature transforming, and heat source method. The detailed information regarding these methods is not given herein since the scope of the study is not evaluation of different methods, and can be found in the literature (Liu et al., 2014). In this study, the heat source method from the fixed grid methods is employed due to its simple, convenient, and easy-to-program nature. In this method, the latent heat of the material is treated as a source term in the governing equation (Al-Saadi & Zhai, 2015). Considering the specific heat and latent heat of the material is combined, the energy equation can be written as given in Equation (2.4).

$$\rho \frac{\partial h}{\partial t} = \frac{\partial}{\partial x}\left(k \frac{\partial T}{\partial x}\right) \tag{2.4}$$

Here, the enthalpy of the material is denoted by h and can be separated into sensible and latent heat components (Equation (2.5)). It should be noted that the sensible heat of the phase changing material is taken as constant (Table 2.1).

$$\frac{\partial h}{\partial t} = \frac{\partial h}{\partial T}\frac{\partial T}{\partial t} = \left(\rho c_p + \rho L_H \frac{\partial f}{\partial T}\right)\frac{\partial T}{\partial t} = \rho c_p \frac{\partial T}{\partial t} + \rho L_H \frac{\partial f}{\partial T}\frac{\partial T}{\partial t} \tag{2.5}$$

This equation (Equation (2.5)) is substituted into Equation (2.4), and the resulting equation is arranged as follows where the latent heat component of the material appears as a source term (Equation (2.6)):

$$\rho c_p \frac{\partial T}{\partial t} = \frac{\partial}{\partial x}\left(k \frac{\partial T}{\partial x}\right) - \rho L_H \frac{\partial f}{\partial t} \tag{2.6}$$

where, L_H represents the latent heat capacity of the phase change material. The f in the given equation denotes the liquid fraction and the value of this parameter ranges between 0 and 1. The unity (f = 1) means that the PCM is completely liquid whereas zero (f = 0) means that the PCM is completely solid. When the value of liquid fraction is between 0 and 1 ($0 < f < 1$), it means that the PCM region is in mushy zone. Besides, it should be noted that the temperature of PCM undergoing phase transition is constant during the phase change process under the assumption that the phase change occurs isothermally, i.e., at a certain temperature (T_f).

The corresponding boundary conditions at the interior and exterior surface of the considered composite wall are given in Equation (2.7) and Equation (2.8), respectively.

$$-k \frac{\partial T}{\partial x}\Big|_{x=0} = h_{in}\left(T_{room} - T_{wall,in}(t)\right) \tag{2.7}$$

$$-k \frac{\partial T}{\partial x}\Big|_{x=L} = h_{out}\left(T_{wall,out}(t) - T_{sol-air}(t)\right) \tag{2.8}$$

Here, h_{in} and h_{out} are the convective heat transfer coefficients for the interior and exterior surfaces. Heat transfer occurs by natural convection between the interior surface of the wall and the room while it occurs by forced convection between the exterior surface of the wall and outdoor. The heat transfer coefficients are taken as h_{in} = 7.70 W/(m^2·K) and h_{out} = 25.0 W/(m^2·K) according to Turkish standards given in TS825 (Turkish Standard: Thermal Insulation Requirements for Buildings (TS 825), 2013). The surface temperatures for interior and exterior are represented by $T_{wall,in}$ and $T_{wall,out}$. The room temperature is denoted by T_{room} and taken as constant (22 ℃) throughout the thermal analyses. The total length of the wall in the *x*-direction is depicted by L. The solar-air temperature is utilized for the outdoor boundary condition, and denoted by $T_{sol\text{-}air}$ and the regarding equation is given in Equation (2.9) (Asan & Sancaktar, 1998).

$$T_{sol-air}(t) = \frac{|T_{max} - T_{min}|}{2} \sin\left(\frac{2\pi t}{P} - \frac{\pi}{2}\right) + \frac{|T_{max} - T_{min}|}{2} + T_{min} \tag{2.9}$$

The solar-air temperature fluctuates between T_{max} and T_{min} during one-day (24 h) period which is represented by P. The upper and lower limits of the solar-air temperature are chosen as 40 ℃ and 0 ℃, respectively, to maximize the utilization of latent heat capacity. It should be noted that the solar-air temperature range considered in the study is hypothetical and used for the sake of exploitation of latent heat at the highest possible rate although it is known that in practical applications, the daily cycles of melting and solidification cannot be ensured perfectly. The considered daily solar-air temperature profile for the outdoor boundary condition is given in Figure 2.4.

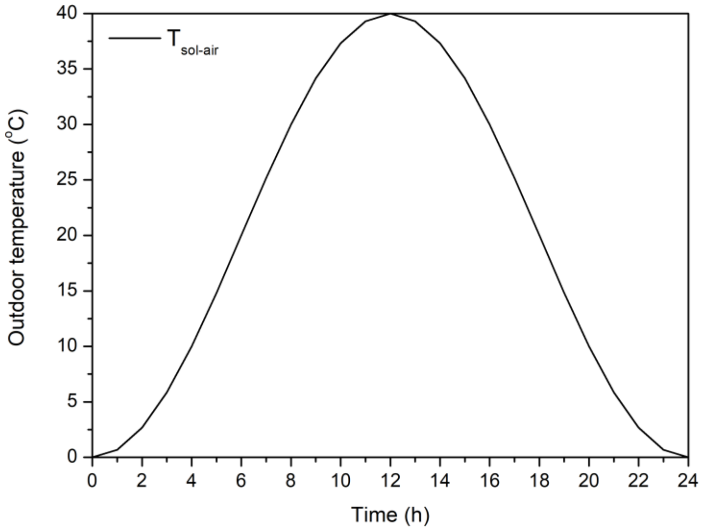

Figure 2.4. The solar-air temperature fluctuation

2.3. Discretization of the Governing Equations

The governing equation of the problem must be discretized to obtain a system of linear equations so it can be solved. In discretization of differential equation appearing in the mathematical modeling of the problem, one of the well-known approaches, i.e., finite difference method, is employed. In order to represent the governing equation by discrete points, problem domain is split into finite number of elements as shown in Figure 2.5.

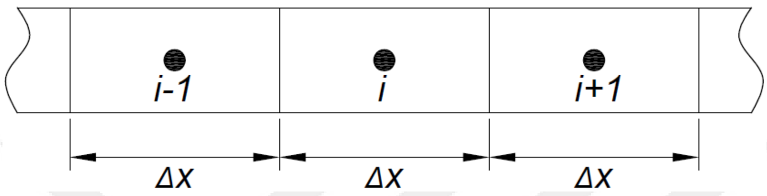

Figure 2.5. The discretized problem domain

Here, *i* represents the modelled node while *i – 1* and *i + 1* represent the neighboring points on the left and right side, in spatial coordinates. Then, the finite difference approximation to first derivative of an arbitrary function (u) can be utilized as in Equation (2.10), through using Taylor Series expansion.

Forward difference approximation:

$$\frac{du}{dx} \approx \frac{u(x+\Delta x)-u(x)}{\Delta x} \equiv \frac{u_{i+1}-u_i}{\Delta x} \tag{2.10a}$$

Backward difference approximation:

$$\frac{du}{dx} \approx \frac{u(x)-u(x-\Delta x)}{\Delta x} \equiv \frac{u_i-u_{i-1}}{\Delta x} \tag{2.10b}$$

Central difference approximation:

$$\frac{du}{dx} \approx \frac{u(x+\Delta x)-u(x-\Delta x)}{2\Delta x} \equiv \frac{u_{i+1}-u_{i-1}}{2\Delta x} \tag{2.10c}$$

Therefore, the first derivative of temperature with respect to time in the energy equation can be approximated as follows by applying forward finite difference in temporal coordinates (Equation (2.11)).

$$\frac{\partial T}{\partial t} \approx \frac{T_i^{n+1} - T_i^n}{\Delta t} \tag{2.11}$$

Here, the superscript *n* represents the points in temporal coordinates while *Δt* depicts the time step size. Similarly, the first derivative of liquid fraction with respect to time, i.e., appears as a source term in Equation (2.6), is approximated and given in Equation (2.12).

$$\frac{\partial f}{\partial t} \approx \frac{f_i^{n+1} - f_i^n}{\Delta t} \tag{2.12}$$

The second derivative of temperature with respect to spatial coordinate (*x*), can be approximated with central finite difference as follows while the explicit scheme is employed (Equation (2.13)).

$$\frac{\partial}{\partial x}\left(\frac{\partial T}{\partial x}\right) \approx \frac{\left(\frac{\partial T}{\partial x}\right)_{i+\frac{1}{2}} - \left(\frac{\partial T}{\partial x}\right)_{i-\frac{1}{2}}}{\Delta x} = \frac{1}{\Delta x}\left(\frac{T_{i+1}^n - T_i^n}{\Delta x} - \frac{T_i^n - T_{i-1}^n}{\Delta x}\right) \tag{2.13}$$

By rearranging (Equation (2.14)):

$$\frac{\partial}{\partial x}\left(\frac{\partial T}{\partial x}\right) \approx \frac{T_{i+1}^n - 2T_i^n + T_{i-1}^n}{\Delta x^2} \tag{2.14}$$

where, *Δx* is the step size in spatial coordinates. Therefore, by substituting these approximations in Equation (2.2) and Equation (2.6), the resulting algebraic equations for the energy equation can be obtained, respectively (Equation (2.15)).

$$\rho c_p \left(\frac{T_i^{n+1} - T_i^n}{\Delta t}\right) = k\left(\frac{T_{i+1}^n - 2T_i^n + T_{i-1}^n}{\Delta x^2}\right) \tag{2.15a}$$

$$\rho c_p \left(\frac{T_i^{n+1} - T_i^n}{\Delta t}\right) = k\left(\frac{T_{i+1}^n - 2T_i^n + T_{i-1}^n}{\Delta x^2}\right) - \rho L_H \left(\frac{f_i^{n+1} - f_i^n}{\Delta t}\right) \tag{2.15b}$$

Since the explicit scheme is employed in the discretization process, these algebraic equations can be directly solved once the stability criterion is ensured, i.e., Fourier Number (*Fo*) lower than 0.5. The stability criteria for the internal and boundary nodes are respectively given in Equation (2.16).

$$Fo = \frac{\alpha \Delta t}{\Delta x^2} \leq 0.5 \tag{2.16a}$$

$$Fo = \frac{\alpha \Delta t}{\Delta x^2} \leq \frac{1}{2(Bi + 1)} \tag{2.16b}$$

Here, α represents the thermal diffusivity of material and Bi stands for Biot Number, and they are defined as follows (Equation (2.17)).

$$\alpha = \frac{k}{\rho c_p} \tag{2.17a}$$

$$Bi = \frac{h\,\Delta x}{k} \tag{2.17b}$$

The discretized governing equation is solved by an in-house code developed in Fortran programming language to obtain temperature field. The next section describes the validation of the developed numerical code with respect to analytical solution along with an experimental work.

2.4. Validation of the Model

Prior to the validation of the developed numerical code, the grid size independence test is carried out for different grid sizes in spatial coordinates. In this context, the 24-h behavior of average liquid fraction is plotted for grid sizes of Δx = 0.5 mm, 1 mm, 2 mm, and 4 mm, and the obtained results are given in Figure 2.6. It should be noted that the stability criterion is always satisfied during the grid size independence study. As can be seen in the given figure, the average liquid fraction changes so little for the 0.5 mm grid size compared to 1 mm grid size meaning that the truncation error can be neglected. Therefore, Δx = 1 mm is chosen for the thermal analyses in the developed numerical code. The corresponding time step ($\Delta t \cong 0.35$ s) is chosen while ensuring the Fourier number is less than the criteria meaning that the numerical scheme is stable. The daily liquid fraction evaluation is observed for different values of *Fo* number (*Fo* = 0.10, 0.25 and 0.50) while the spatial grid size is kept constant and found no significant variation.

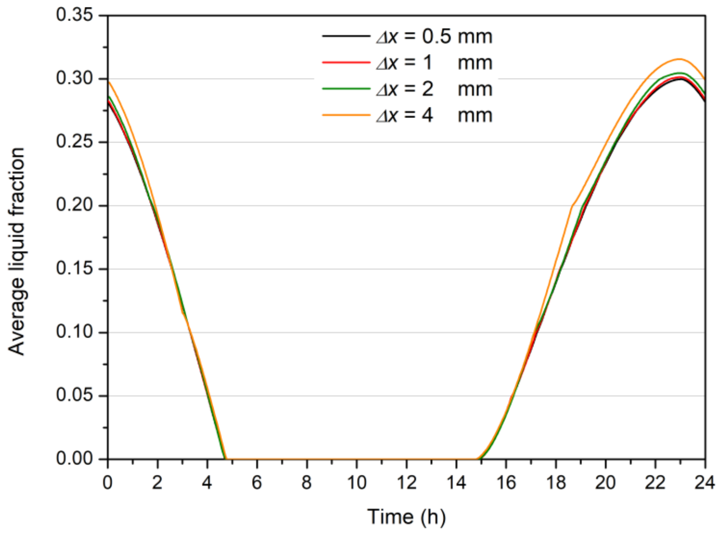

Figure 2.6. Grid independence test for Δx = 0.5 mm, 1 mm, 2 mm, and 4 mm

First of all, the developed numerical code for thermal analyses is verified with analytical solution of melting and solidification. Then, an experimental work published is used to verify the model. The analytical approach is called Neumann's solution considering melting or solidification of a semi-infinite region which initially at solid or liquid state, respectively (Jiji, 2000; Özışık, 1980). It can be seen in the literature that the phase change problem also is called as Stefan's problem, and the corresponding solution is called Stefan's solution. However, Neumann's solution of the phase change is a more general problem than Stefan's problem which can be considered as a special case within Neumann's solution. The assumptions made in Neumann's solution are as follows (Jiji, 2000):

- Heat conduction is one-dimensional.
- Thermophysical properties are constant and uniform for each phase.
- The convection of fluid is neglected.

Considering these assumptions, the equations used for analytical solution during melting process are given below (Jiji, 2000). Interphase position (x_i) is given in Equation (2.18):

$$x_i = \lambda\sqrt{4\alpha_l t} \tag{2.18}$$

where, λ stands for a constant to be determined and α_l depicts the thermal diffusivity in liquid phase. The temperature in liquid phase can be calculated with Equation (2.19):

$$T_l(x,t) = T_0 + \frac{(T_f - T_o)}{\text{erf}(\lambda)}\text{erf}\left(\frac{x}{\sqrt{4\alpha_l t}}\right) \quad (2.19)$$

where, T_f and T_0 represent the fusion temperature (also known as melting temperature or phase transition temperature) and surface temperature, respectively. The temperature in solid phase can be calculated from Equation (2.20):

$$T_s(x,t) = T_i + \frac{(T_f - T_i)}{1 - \text{erf}(\sqrt{\alpha_l/\alpha_s}\lambda)}\left(1 - \text{erf}\left(\frac{x}{\sqrt{4\alpha_s t}}\right)\right) \quad (2.20)$$

where, T_i represents the initial temperature and α_s depicts the thermal diffusivity in solid phase. Therefore, the constant λ can be determined by using the following equation (Equation (2.21)).

$$\frac{\exp(-\lambda^2)}{\text{erf}(\lambda)} - \sqrt{\frac{\alpha_l}{\alpha_s}}\frac{k_s}{k_l}\left(\frac{T_f - T_i}{T_0 - T_f}\right)\frac{\exp(-\lambda^2\alpha_l/\alpha_s)}{1 - \text{erf}(\sqrt{\alpha_l/\alpha_s}\lambda)} = \frac{\sqrt{\pi}L_H\lambda}{c_{pl}(T_o - T_f)} \quad (2.21)$$

Similarly, the analytical solution equations used during the solidification process are given below (Jiji, 2000). Interphase position (x_i) is given in Equation (2.22):

$$x_i = \lambda\sqrt{4\alpha_s t} \quad (2.22)$$

The temperature in solid phase can be calculated with Equation (2.23):

$$T_s(x,t) = T_0 + \frac{(T_f - T_o)}{\text{erf}(\lambda)}\text{erf}\left(\frac{x}{\sqrt{4\alpha_s t}}\right) \quad (2.23)$$

The temperature in liquid phase can be calculated from Equation (2.24):

$$T_l(x,t) = T_i + \frac{(T_f - T_i)}{1 - \text{erf}(\sqrt{\alpha_s/\alpha_l}\lambda)}\left(1 - \text{erf}\left(\frac{x}{\sqrt{4\alpha_l t}}\right)\right) \tag{2.24}$$

And finally, the constant λ can be determined by using the equation below (Equation (2.25)).

$$\frac{\exp(-\lambda^2)}{\text{erf}(\lambda)} - \sqrt{\frac{\alpha_s}{\alpha_l}}\frac{k_l}{k_s}\left(\frac{T_i - T_f}{T_f - T_0}\right)\frac{\exp(-\lambda^2\alpha_s/\alpha_l)}{1 - \text{erf}(\sqrt{\alpha_s/\alpha_l}\lambda)} = \frac{\sqrt{\pi}L_H\lambda}{c_{ps}(T_f - T_0)} \tag{2.25}$$

In order to validate the numerical model developed with the analytical solution, both the melting and solidification of a semi-infinite PCM slab is considered. For the melting process, the PCM slab is initially at T_i = 15 °C and the surface temperature is T_0 = 40 °C. For the solidification process, the PCM slab considered to be at T_i = 25 °C and the surface temperature is taken T_0 = 0 °C. The following properties are taken for phase changing material during the validation with analytical solution. The density, specific heat, and thermal conductivity of the material is 820 kg/m^3, 2000 J/(kg·K), and 0.2 W/(m·K), respectively. The melting temperature is T_f = 20 °C while the latent heat capacity is 134×10^3 J/kg.

Based on the assumptions made and the problem description given, the analytical solution for semi-infinite PCM slab is performed by considering for both melting and solidification process. Furthermore, the temperature profiles at different times namely, 5h, 10h, and 20h, are calculated to see if a discrepancy occurs as time moves forward. Meanwhile, the developed numerical code is adopted to simulate the defined problem and the temperature profiles are also obtained at the same times. The temperature profiles determined are comparatively given with respect to location in PCM slab for both melting and solidification in Figure 2.7. It is clear from Figure 2.7a that the analytical solution and the numerical solution is in great agreement during the melting process.

Similarly, the same comment is valid for the solidification process since a great agreement is also observed (Figure 2.7b) between the analytical and numerical solutions during solidification process. It is seen that the numerical code developed can be trusted for modeling of solid-liquid phase changing phenomena. Besides, another validation is also conducted by considering an experimental work to test the validity of the numerical model under more complex boundary conditions which cannot be solved analytically.

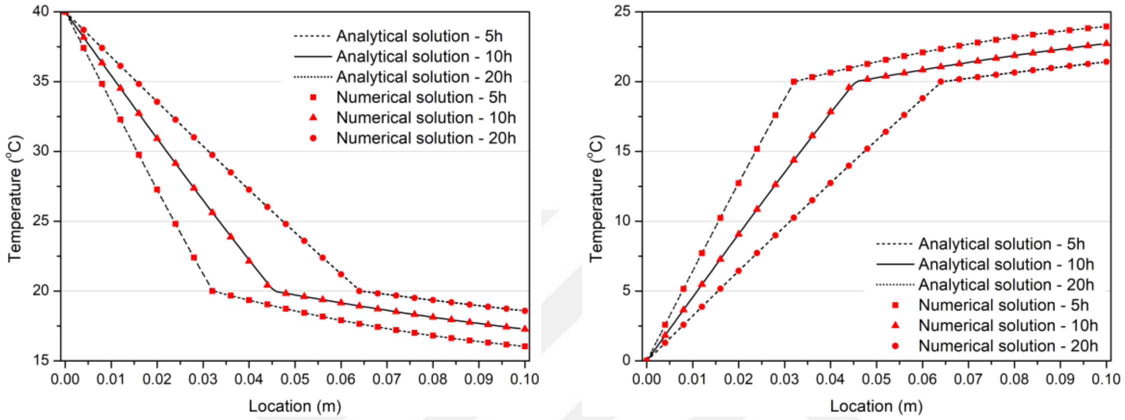

a) b)

Figure 2.7. The validation of the numerical code with analytical solution. a) Validation with analytical solution of melting at various times, b) Validation with analytical solution of solidification at different times

In this context, an experimental study carried out by Fadl et al. (Fadl & Eames, 2019) is chosen as validation of the numerical model. They studied the melting process of PCM (RT44HC) whose thermophysical properties are adopted in the numerical model for validation. The used container in the study is rectangular and its sizes are reported as 100 mm × 200 mm × 200 mm. The liquid fraction behavior of RT44HC during 10h period is plotted for both experimental study and 2-dimensional numerical model in Figure 2.8. It is noted from the graph that the obtained results are in good agreement especially for the first 5h to 6h period. Then, a slight deviation between the experimental data and numerical result can be seen which can be explained by the effect of convection currents in the liquid phase PCM. Since the numerical code developed does not account the convection of molten PCM, the heat transfer in the simulation is lower compared to that of the experimental setup resulting a lower liquid fraction. However, the discrepancy between the liquid fraction values still does not exceed 5 % even after 5h.

After the validation, the 1-dimensional and 2-dimensional numerical models for the PCM containing wall are compared and no significant variation is observed. Therefore, further thermal analyses are carried out by the 1-dimensional model for the sake of computation time. Consequently, the established numerical model can be used for further thermal analyses considering verifications done by the analytical solution and experimental data, separately.

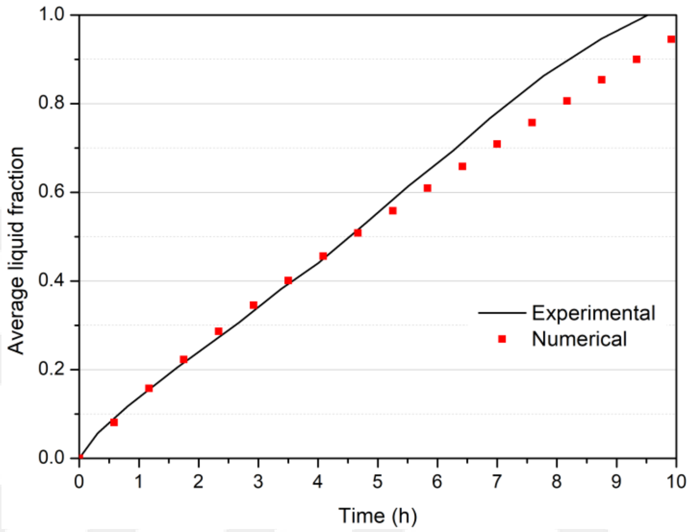

Figure 2.8. The validation of the numerical code with experimental data

2.5. PCM Performance Evaluation Methods and Corresponding Definitions

Depending on the literature review, the existing PCM thermal performance evaluation methodologies for building external wall utilization are gathered and examined. Three representative approaches/methods are determined and named as Method-1, Method-2, and Method-3 with abbreviations of M1, M2, and M3, respectively. The detailed definitions and related formulas for each considered approach are given separately in the upcoming sections.

2.5.1. Method-1

In most of the studies in the literature, the thermal performance of PCM integrated building external wall is evaluated based on the overall energy saving effect that can be reached by utilizing PCM. Therefore, M1 is chosen as a representative approach to these kinds of evaluation techniques which energy saving is the critical parameter. The energy saving due to the integration of PCM is obtained as follows (Equation (2.26)):

$$E_{PCM}(L_{PCM}, T_f) = Q_{Reference} - Q_{PCM}(L_{PCM}, T_f) \quad (2.26)$$

where, E_{PCM} stands for energy saving due to PCM integration while Q for energy demand of the building. The subscripts Reference and PCM represents the reference building wall and PCM integrated building wall, respectively. The required energy to maintain the indoor thermal comfort is calculated according to the given equation (Equation (2.27)). It should be noted that there is no separation as heating or cooling energy demand, but rather only the total energy demand needed to maintain indoor thermal comfort is considered. Therefore, the absolute sign is used in the equation below. For all of the considered cases, namely, Q_{PCM}, $Q_{Reference}$, and Q_{PSM}, the below equation is used to calculate energy demand required.

$$Q = \int_0^P h_{in} |T_{room} - T_{wall}(t)| dt \quad (2.27)$$

The case study is constructed as an optimization study for PCM melting temperature and PCM amount (through PCM layer thickness), thus, an objective function is adopted as given in Equation (2.28).

$$E_{opt}(L_{PCM}, T_f) = max[Q_{Reference} - Q_{PCM}(L_{PCM}, T_f)] \rightarrow L_{PCM,opt}, T_{f,opt} \quad (2.28)$$

Here, E_{opt} is the maximum energy saving of which the term $[Q_{Reference} - Q_{PCM}(L_{PCM}, T_f)]$ is maximized for values of PCM thickness (L_{PCM}) and melting point (T_f). This objective function enables to find the optimum thickness ($L_{PCM,opt}$) and/or optimum phase change temperature ($T_{f,opt}$).

2.5.2. Method-2

It is noted from the literature review that the parameters such as time lag, decrement factor, and total heat gain are also broadly preferred by researchers to evaluate thermal performance of PCM integrated building external walls. In this context, Bhamare et al. (Bhamare et al., 2021) proposed a novel index which combines all of these thermal performance evaluation parameters an named it as MKR index.

Therefore, this proposed index is chosen to evaluate thermal performance in the considered case study and optimize the PCM parameters (PCM thickness, i.e., amount and PCM melting temperature). The time lag (ϕ) is defined as (Equation (2.29)):

$$\phi = \begin{cases} t_{T_{wall,in}^{max}} > t_{T_{wall,out}^{max}} \rightarrow t_{T_{wall,in}^{max}} - t_{T_{wall,out}^{max}} \\ t_{T_{wall,in}^{max}} < t_{T_{wall,out}^{max}} \rightarrow t_{T_{wall,in}^{max}} - t_{T_{wall,out}^{max}} + P \\ t_{T_{wall,in}^{max}} = t_{T_{wall,out}^{max}} \rightarrow P \end{cases} \tag{2.29}$$

where, $t_{T_{wall,in}^{max}}$ and $t_{T_{wall,out}^{max}}$ represents the time in which the interior and exterior surface temperatures are reached at their maximum values, respectively. The decrement factor (f_D) is defined as given in Equation (2.30).

$$f_D = \frac{T_{wall,out}^{max} - T_{wall,out}^{min}}{T_{wall,in}^{max} - T_{wall,in}^{min}} \tag{2.30}$$

Here, $T_{wall,out}^{max}$ and $T_{wall,out}^{min}$ represents the maximum and minimum temperatures on the exterior surface of the wall, respectively. Besides, $T_{wall,in}^{max}$ and $T_{wall,in}^{min}$ denotes the maximum and minimum temperatures on the interior surface of the wall, respectively. Therefore, it can be said that the numerator represents the amplitude of temperature on the exterior surface while the denominator represents the amplitude of temperature on the interior surface of the external wall. According to the considered index, the time lag, decrement factor and total heat gain are nondimensionalized by their counterparts which are in the reference case, i.e., without PCM (Equation (2.31)):

$$\phi'(L_{PCM}, T_f) = \frac{\phi_{PCM}(L_{PCM}, T_f)}{\phi_{Reference}} \tag{2.31a}$$

$$f_D'(L_{PCM}, T_f) = \frac{f_{D,PCM}(L_{PCM}, T_f)}{f_{Reference}} \tag{2.31b}$$

$$Q'(L_{PCM}, T_f) = \frac{Q_{PCM}(L_{PCM}, T_f)}{Q_{Reference}} \tag{2.31c}$$

Here, the parameters ϕ', f_D' and Q' shows the dimensionless time lag, decrement factor and total heat gain, respectively. The total heat gain is already defined as the required energy demand in Equation 2.27, so it is not defined here again. Based on these dimensionless parameters, the index is offered as given in Equation (2.32).

$$MKR(L_{PCM}, T_f) = \frac{f_D'(L_{PCM}, T_f)}{[\phi'(L_{PCM}, T_f) + c]Q'(L_{PCM}, T_f)} \quad (2.32)$$

Here, the parameter c is a constant value to avoid obtaining extremely high values for the index and taken as 0.5 in the simulations. The objective function for this approach is defined as in Equation (2.33).

$$MKR_{opt}(L_{PCM}, T_f) = max[MKR(L_{PCM}, T_f)] \rightarrow L_{PCM,opt}, T_{f,opt} \quad (2.33)$$

Here, MKR_{opt} stands for maximum MKR index of which the MKR index is maximized for the values of PCM thickness (L_{PCM}) and melting point (T_f).

2.5.3. Method-3

There are studies in the literature considering the latent heat utilization impact on the energy saving amount of PCM integration to building external wall (Arıcı et al., 2020; Izquierdo-Barrientos et al., 2012; Mazzeo et al., 2017; Tunçbilek, Arıcı, Krajčík, et al., 2020). However, this aspect of PCM is not well studied, therefore there are few studies focused on and highlighted the latent heat contribution in energy saving. On the other hand, it is important to note that this aspect of PCM utilization is obviously the most prominent and dominant feature of using PCM in building external walls since a great deal of thermal energy can be stored/extracted depending on the outdoor conditions. Furthermore, latent heat capacity is the major parameter separating PCM from an insulation material considering the building wall applications. Therefore, this method (M3) aims to maximize the benefit of PCM integration by focusing on the latent heat contribution on the energy saving. In order to separate the effect of latent heat effect from the sensible heat effect on the energy saving, a case with PCM but with inability to phase change is considered. This case is named PSM as already mentioned in the literature review section. The PSM layer is always at the same thickness with PCM layer and has the same thermophysical properties. However, this case (PSM) does not undergo phase change meaning that latent heat cannot be utilized in the energy saving. Therefore, the energy saving for PSM can be calculated as follows (Equation (2.34)):

$$E_{PSM}(L_{PSM}) = Q_{Reference} - Q_{PSM}(L_{PSM}) \quad (2.34)$$

Here, E_{PSM} and Q_{PSM} represent the energy saving and energy demand due to PSM integration to the building external wall. In this case, the energy saving due to latent heat exploitation can be expressed as the subtraction of E_{PCM} and E_{PSM}. This approach is rather straightforward but also logical since E_{PCM} also contains the E_{PSM}. The term E_{PSM} herein can be considered as the energy saving due to increased thermal mass and thermal resistance of the wall. Therefore, the energy saving due to only latent heat utilization (E_{LH}) is given by Equation (2.35) as follows.

$$E_{LH}(L_{PSM}, T_f) = E_{PCM}(L_{PCM}, T_f) - E_{PSM}(L_{PSM}) \quad (2.35)$$

The objective function adopted to optimize PCM layer thickness and melting temperature is given in Equation (2.36). It should be noted that L_{PCM} and L_{PSM} are the same thickness values in the below equation.

$$E_{opt}\left(L_{PCM/PSM}, T_f\right) = max\left[E_{PCM}\left(L_{PCM}, T_f\right) - E_{PSM}(L_{PSM})\right] \rightarrow L_{PCM,opt},\ T_{f,opt} \quad (2.36)$$

3. RESULTS AND DISCUSSION

The results and related discussions are consisted of three separate sections named 3.1. PCM Thermal Performance Evaluation with Different Approaches, 3.2. Thermal Performance of PCM Utilization Compared to Insulation, and 3.3. Thermal Impact of Combination of PCM and Insulation on Energy Saving. Each section is also divided into subsections to convey the discussion and obtained findings clearly.

3.1. PCM Thermal Performance Evaluation with Different Approaches

One of the most important parameters affecting the thermal performance of PCM application is obviously the phase change temperature of the PCM since the latent heat utilization is completely dependent on this parameter. As the effect of PCM layer merely an insulation material without the latent heat exploitation, it is crucial to use latent heat through phase change process (both melting and solidification). Therefore, in order to gain the best thermal performance from the PCM integration to the composite building external wall, 16 different phase change temperatures ranging between 15 °C and 30 °C (by 1 °C increment) are tested. Besides, different PCM layer thicknesses, i.e., PCM amounts, are located inside the composite wall to find the optimum PCM layer thickness (if exists), i.e., the thickness is varied from 2 mm to 40 mm (by 2 mm increment). It is important to note that the optimum phase change temperature can change depending on the PCM layer thickness also due to varying thermal resistance of PCM layer inside the composite wall as different thicknesses are utilized. Therefore, the corresponding optimum phase change temperature is found along with each considered PCM layer thickness. Furthermore, since the thermal behavior and optimum values for other design parameters namely PCM layer thickness and phase transition temperature can change depending on the location of PCM inside the wall, the PCM layer is located either near the indoor or near the outdoor environment.

As previously pointed out, three methods are determined based on the existing literature and defined to evaluate the thermal performance of PCM integrated external building wall. Herein, the optimization of PCM phase transition temperature, layer thickness and location inside the wall are performed and the obtained results are discussed for three considered methods.

3.1.1. Method-1 (M1)

Since this method evaluates the thermal performance of PCM integration to the external building wall based on the energy saving, energy saving values (E_{PCM}) due to PCM integration for each considered PCM case are calculated. In order to give a perspective on the variation of energy saving with respect to each phase change temperature and find the optimum value, four PCM layer thicknesses namely 10 mm, 20 mm, 30 mm, and 40 mm are selected and shown in Figure 3.1. Besides, the obtained results are given for both PCM located near the indoor (Figure 3.1a) and near the outdoor (Figure 3.1b). In the case of without PCM layer, which is also called as the reference case, the energy demand is calculated as 1124.3 kJ/m^2 per day. As can be seen from the figures, PCM integration can reduce the energy demand of the room significantly depending on the phase change temperature. The melting temperature greatly affects the energy demand of the room (Figure 3.1a), and an optimum value exists for the melting temperature of PCM. According to the results obtained, the optimum phase change temperatures are found as 22 ℃ regardless of the PCM layer thickness. This result can be expected since the PCM layer is located near the indoor, and the indoor temperature is kept as constant in 22 ℃. Furthermore, there are several studies in the literature underlying the same conclusion. It is seen from the figure that no phase change occurs, therefore no latent heat is used, for the melting temperatures between 15 ℃ – 18 ℃ and 24 ℃ – 30 ℃. However, still a great amount of energy saving occurs due to the thermal resistance and thermal mass of the PCM layer. Remaining melting temperatures (19 ℃, 20 ℃, 21 ℃, 22 ℃ and 23 ℃) enable phase change and therefore a great amount of energy saving is observed for all of the shown PCM layer thicknesses. It is shown that the energy saving (E_{PCM}) increases gradually towards to the optimum melting temperature. For instance, considering 20 mm PCM layer thickness, energy saving is determined as 392.6 kJ/m^2, 433.1 kJ/m^2, 547.1 kJ/m^2, 716.9 kJ/m^2, 759.3 kJ/m^2, 478.4 kJ/m^2, and 398.3 kJ/m^2 for phase change temperatures of 18 ℃, 19 ℃, 20 ℃, 21 ℃, 22 ℃, 23 ℃, and 24 ℃, respectively. A similar pattern is also observed for other considered PCM layer thickness values. The maximum energy saving with 22 ℃ melting temperature is determined as 716.2 kJ/m^2, 759.3 kJ/m^2, 794.1 kJ/m^2, and 822.9 kJ/m^2 for 10 mm, 20 mm, 30 mm, and 40 mm, respectively. When PCM is located near the outdoor, the optimum melting temperature varies significantly as can be seen in Figure 3.1b.

This outcome obviously can be explained by the fact that it is more susceptible to the changes in the outdoor climatic conditions since PCM layer is close to the exterior environment. Therefore, finding an optimum melting temperature is rather difficult compared to the case of PCM located near the interior environment. Furthermore, this phenomenon is more obvious for the lower PCM layer thickness values such as observed in the case of 10 mm. The energy saving values (E_{PCM}) for 10 mm depending on the melting temperature fluctuates only between 337.7 kJ/m^2 and 405.3 kJ/m^2 whereas this fluctuation is between 232.6 kJ/m^2 and 716.2 kJ/m^2 in the case of PCM located near the indoor (for 10 mm also). This result indicates that the selection of appropriate phase change temperature for PCM integration to the external wall is more significant when the PCM is located near the indoor compared to near the outdoor. Although the energy saving values are very close to each other, a phase change temperature providing the highest energy saving is found as 18 °C with 405.3 kJ/m^2 for 10 mm PCM layer thickness. Apparently, when the PCM layer thickness is increased, the energy saving values are increased and the temperature value giving the least demand varies also. For instance, energy saving is calculated as 691.6 kJ/m^2, 793.9 kJ/m^2, and 822.7 kJ/m^2 for 20 mm, 30 mm, and 40 mm. The corresponding optimum phase change temperatures for these values are 21 °C, 22 °C, and 23 °C, respectively. From a broad perspective, it is noted that the location of the PCM layer is only significant when the PCM layer thickness is lower. Otherwise, the thickness of PCM layer has no substantial effect on the energy demand and therefore energy saving. For instance, locating PCM layer near the indoor is more beneficial in terms of energy saving for the PCM layer thicknesses of 10 mm and 20 mm compared to locating it near the outdoor. However, considering the layer thicknesses of 30 mm and 40 mm, locating PCM layer either near the indoor or outdoor has no significant effect on energy demand since they provide almost the same energy saving values at their optimal melting temperatures.

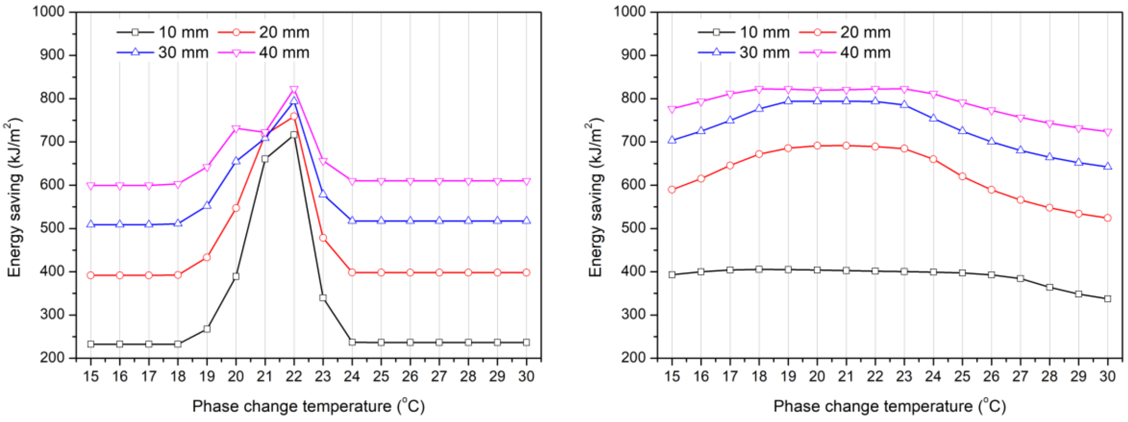

a) b)

Figure 3.1. Energy saving amount with respect to phase change temperature for selected PCM thicknesses (Method-1). a) PCM located near indoor (C1), b) PCM located near outdoor (C2)

Based on the energy saving, optimum phase change temperature for all of the considered PCM layer thicknesses is calculated and given in Figure 3.2. As can be seen from the given figure, optimum phase change temperature which provides the highest possible energy saving is found as 22 °C for all of the considered PCM layer thicknesses when the PCM layer is located near the interior environment. This can be explained by the fact that the PCM layer is very close to the indoor and the indoor temperature is kept constant at the room temperature (22 °C). Contrary, it can be expected that the optimum phase change temperature of PCM layer located close to the outdoor varies depending on the layer thickness. As expected, the optimum phase change temperature greatly differs from the PCM layer thickness 2 mm to 40 mm. A general increasing trend in the optimum phase change temperature is observed from lower to higher PCM layer thicknesses. For instance, it gradually increases from 16 °C to 23 °C depending on the layer thickness. This phenomenon can be justified by the fact that the PCM layer is more susceptible to the changes in the outdoor climatic conditions since it is very close to the exterior environment. Besides, considering only outer plaster thermal resistance and thermal mass at the back of the PCM layer, increasing PCM layer thickness and therefore thermal resistance as well as thermal mass of the PCM layer in the wall results in the radical changes of optimum melting temperature.

Consequently, the optimum phase change temperature is constant and equals to the room temperature when the PCM is located near the indoor regardless of the layer thickness, and it varies greatly when the PCM is located near the outdoor depending on the layer thickness.

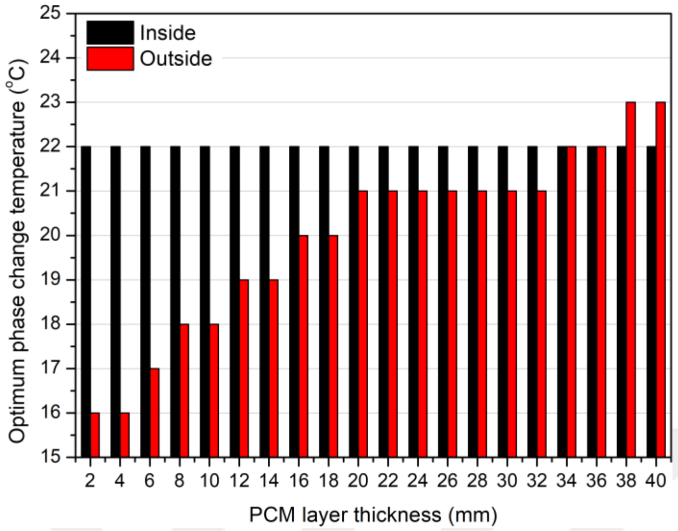

Figure 3.2. Optimum phase change temperature with respect to PCM layer thickness (Method-1)

In order to find an optimum layer thickness for PCM layer, energy saving amounts corresponding to the each PCM layer thickness with the optimum phase change temperature are determined and given in Figure 3.3. As can be seen from the figure, no optimum value occurs for the layer thickness regardless of the PCM location meaning that increasing the PCM layer thickness will always increase the respective energy saving. The energy saving starts from 241.4 kJ/m^2 and reaches up to 822.9 kJ/m^2 for the inside located PCM whereas it starts from 95.4 kJ/m^2 and reaches up to 822.7 kJ/m^2 for the outside located PCM. According to the obtained results, it is noted that the location of the PCM layer is only significant at lower PCM layer thicknesses. As can be seen in the figure, at lower PCM layer thickness values, the energy saving for PCM located near the indoor is substantially higher than that of PCM located near outdoor. However, at higher PCM layer thicknesses especially after 22 mm, the energy saving is almost the same for both PCM located near the outdoor and PCM located near the indoor.

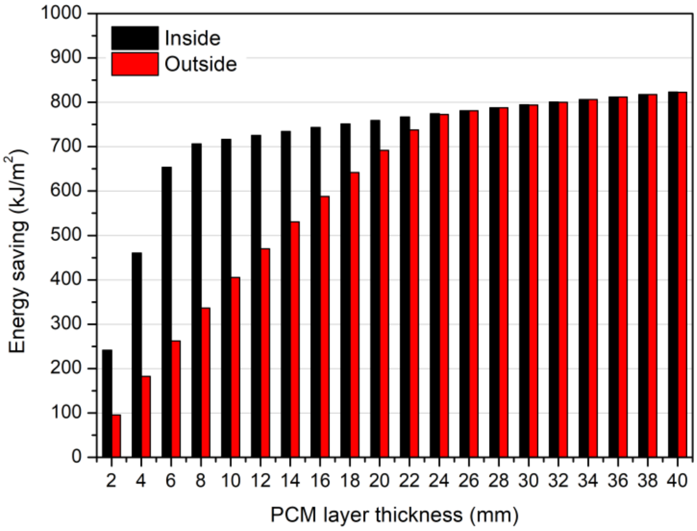

Figure 3.3. Energy saving amount with respect to PCM layer thickness considering optimum melting temperature (Method-1)

According to the discussion presented above, it can be stated that Method-1 gives an optimum melting temperature for each PCM layer thickness, and this value can change for the outside location whereas is constant (T_f = 22 °C) for the inside location. However, an optimum layer thickness i.e., PCM amount, for the PCM layer has not been found since the energy saving always increases as the thickness of the PCM layer is increased.

3.1.2. Method-2 (M2)

Parameters of time lag, decrement factor and total heat gain are the evaluating indicators of PCM integrated building external wall performance in this method. Therefore, for all of the considered phase change temperatures, layer thicknesses and locations, these parameters are calculated. As mentioned previously, these parameters are combined into one index and the evaluation of thermal performance is carried out based on this index. First of all, the obtained MKR indexes with respect to different melting temperatures for 10 mm, 20 mm, 30 mm, and 40 mm are shown in Figure 3.4 to see the variation of the MKR index depending on the phase change temperature. It should be noted that the higher the MKR index, the higher the thermal performance of the PCM integrated wall. As can be seen from Figure 3.4a, MKR index greatly fluctuates depending on the melting temperature regardless of the PCM layer thickness when the PCM is located near the indoor.

The MKR index reaches a highest point for each PCM layer thickness at different phase change temperatures. For instance, the MKR index of 5.0 (10 mm), 7.5 (20 mm), 15.7 (30 mm), and 11.5 (40 mm) are observed at 22 °C, 21 °C, 21 °C, and 22 °C phase change temperatures. It is interesting to note that the highest MKR index of 30 mm layer thickness is higher than that of the highest MKR index of 40 mm layer thickness. This indicates that there is an optimum layer thickness value based on the MKR index thermal performance evaluation, which will be discussed later. However, contrary to the PCM located the indoor, increasing the thickness of PCM layer results in always higher MKR index values in the case of PCM located near the outdoor (Figure 3.4b). Furthermore, it is important to note that the optimum melting temperature for each thickness varies depending on the PCM layer thickness except for the case of 10 mm. According to the obtained results, 24 °C, 23 °C, 22 °C, and 21 °C are the optimum phase change temperatures (T_f) for 10 mm, 20 mm, 30 mm, and 40 mm PCM layer thicknesses, respectively. The corresponding MKR indexes for these cases are calculated as 1.9, 5.6, 11.4, and 18.6. Despite that, the fluctuation of the MKR index with respect to phase change temperature for 10 mm thickness is within rather a small range (MKR = 1.5 to 1.9) compared to other thicknesses. This almost prevents emerging any optimum phase change temperature for 10 mm thickness. Therefore, it can be said that, at low PCM layer thicknesses and PCM located near the outdoor cases, it is difficult to find an optimum phase change temperature for the PCM application.

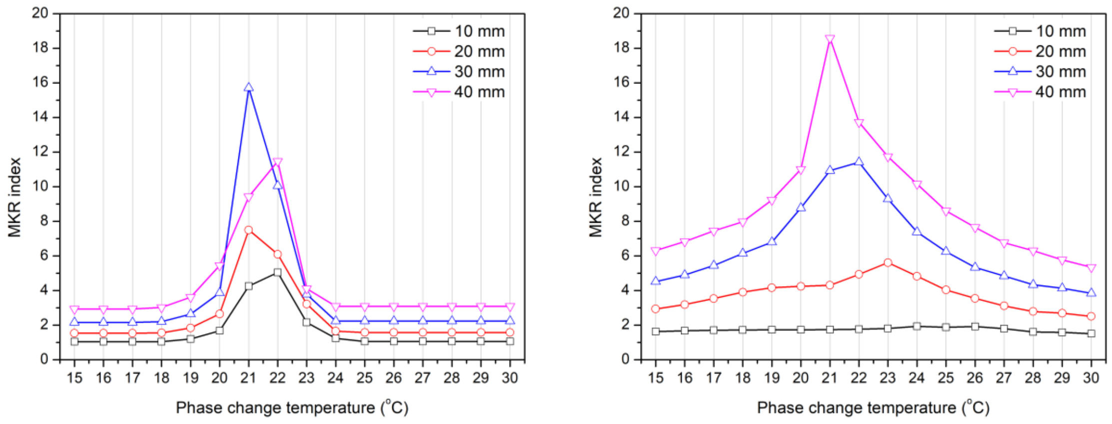

a) b)

Figure 3.4. MKR index with respect to phase change temperature for selected PCM thicknesses (Method-2). a) PCM located near indoor (C1), b) PCM located near outdoor (C2)

Based on the MKR indexes calculated, optimum phase change temperature for each considered PCM layer thickness is obtained and given in Figure 3.5. As can be seen from the given figure, the optimum phase change temperature is highly affected by the thickness of PCM layer. Besides, locating the PCM layer near the indoor or near the outdoor has also great impact on the optimum melting temperature. For instance, in the case of 20 mm PCM layer thickness, the optimum phase change temperature (T_f) is found as 21 °C and 23 °C for the PCM located indoor and outdoor, respectively. A similar phenomenon, i.e., having different optimum melting temperatures for inside and outside locations, is observed for other PCM layer thicknesses expect for the 32 mm and 34 mm (T_f = 21 °C). It is noted that there is a decreasing trend in the optimum melting temperature for the outside location from 26 °C to 21 °C as the thickness of PCM layer is increased. However, such a regular trend cannot be seen for the inside location which the optimum melting temperature is fluctuated between 21 °C to 23 °C. These findings also highlight that the fluctuation of optimum melting temperature with respect to the thickness for outside location is higher than that of inside location. This can be explained by the fact that the PCM located near the outdoor is more susceptible to the changes in outdoor climatic conditions since it is closer to the outdoor environment. It should be noted that the optimum melting temperature for the inside location does not change and found 22 °C regardless of the PCM layer thickness based on energy saving parameter evaluation (Method-1). However, herein (based on the MKR index) the situation is rather different since a fluctuating optimum melting temperature is found for the inside location also. In order to find an optimum layer thickness for PCM layer, the MKR index values corresponding to the each PCM layer thickness with the optimum phase change temperature are given in Figure 3.6. As can be seen from the given figure, the MKR index is observed to be different for locating PCM layer near the indoor or near the outdoor. The index varies between 0.98 and 16.9 for the inside while it varies between 0.84 and 18.6 for the outside. It is interesting to note that the MKR index has highest value at 34 mm layer thickness for the inside location meaning that an optimum layer thickness (PCM amount) exists. However, such a conclusion has not been observed for the outside location. Therefore, it can be said that an optimum layer thickness exists for the inside location whereas does not exist for the outside location.

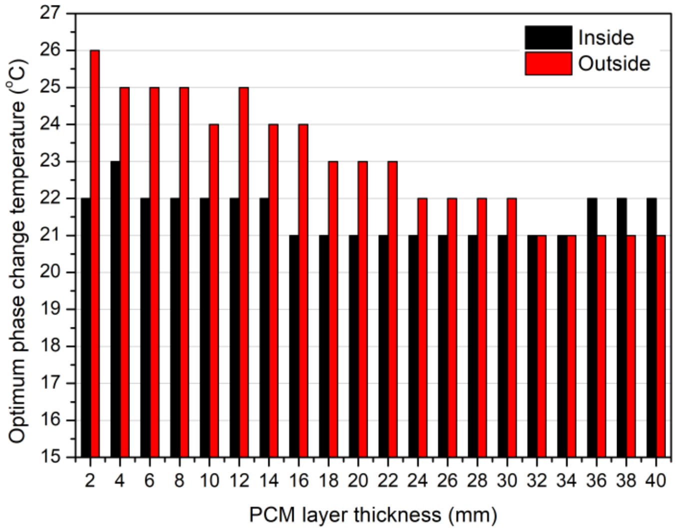

Figure 3.5. Optimum phase change temperature with respect to PCM layer thickness (Method-2)

The highest MKR index is calculated as 16.9 for 34 mm (inside) and as 18.6 for 40 mm (outside). Besides, a gradual increase in the MKR index with respect to the PCM layer thickness is observed for the outside location. In contrary, steep increases and decreases are observed for the inside location whereas only increase is observed for the outside location. For instance, when the thickness is increased from 20 mm to 22 mm, the MKR index jumps from 7.5 to 15.2 where the MKR index is nearly doubled considering the inside location. A radical decrease is observed as the MKR index is reduced from 16.9 to 10.9 for (from 34 mm to 36 mm).

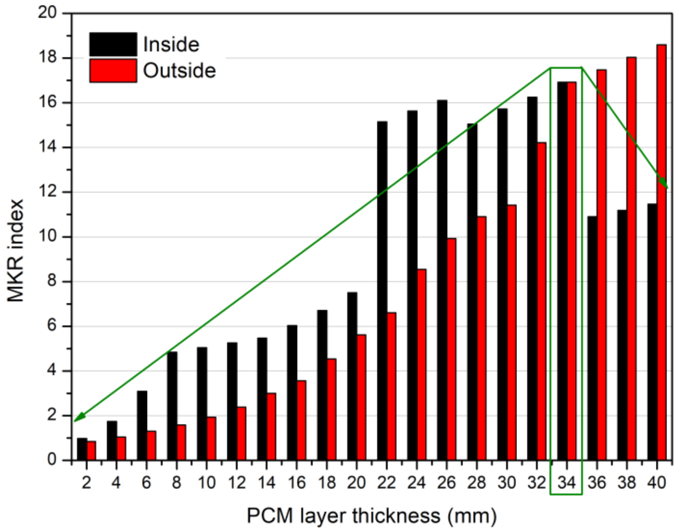

Figure 3.6. MKR index with respect to PCM layer thickness considering optimum melting temperature (Method-2)

Consequently, it is found that optimum value for melting temperature greatly differs based on the location as well as the thickness of PCM layer. An optimum value for the PCM layer thickness (L_{PCM} = 34 mm) is found when the PCM layer is located near the indoor. However, contrary to the inside location, no optimum PCM layer thickness is found for the outside location since the MKR index always increases as the thickness of PCM is increased.

3.1.3. Method-3 (M3)

This method evaluates the thermal performance of PCM integrated building external wall by separating the contribution of latent heat (E_{LH}) on the energy saving from the total energy saving (E_{PCM}) obtained. Therefore, the optimization of melting temperature, PCM layer location and PCM layer thickness is performed based on this parameter, i.e., the contribution of latent heat utilization on energy saving (E_{LH}). To show the variation of energy saving due to latent heat utilization with respect to melting temperature, four PCM layer thicknesses are selected and the corresponding energy saving values (E_{LH}) for each considered phase change temperature as well as the location are given in Figure 3.7. As can be seen in Figure 3.7a, a certain optimum melting temperature occurs for each PCM layer thickness where the energy saving due to latent heat utilization (E_{LH}) reaches a peak value for a certain melting temperature. In this case, the optimum melting temperature is found as 22 ℃ irrespective of the PCM layer thickness. The highest energy saving is obtained for 10 mm (at T_f = 22 ℃) and the amount of the energy saved is 483.5 kJ/m^2. Furthermore, the energy saved by 10 mm PCM layer thickness is nearly two-folds of that 40 mm PCM layer thickness. This clearly shows the significance of latent heat exploitation on energy saving in the PCM integration. The energy saving amount is observed to be decreased as the thickness of the PCM layer increases. For instance, 367.4 kJ/m^2, 285.2 kJ/m^2, and 223.2 kJ/m^2 energy saving is calculated for 20 mm, 30 mm, and 40 mm PCM layer thicknesses, respectively. This finding indicates that there is an optimum PCM layer thickness for the PCM located near the indoor, which will be discussed later. It is important note that the zero values in the figure mean that there is no energy saving due to latent heat exploitation (E_{LH} = 0).

However, that does not mean there is no energy saving at all, which in fact, there is certainly energy saving due to PCM integration ($E_{PCM} = E_{PSM}$ since $E_{LH} = 0$) to the wall which is already discussed previously in Method-1 section. In the case of PCM located near the outdoor, a rather different trend of energy saving with respect to melting temperature is observed (Figure 3.7b). The optimum melting temperature is not so obvious since a parabolic profile of energy saving is seen. Furthermore, the amounts of energy saving for different phase change temperatures are very close to each other especially for the melting temperatures around 21 °C. Despite that, there is an optimum melting temperature for each thickness. For instance, 18 °C, 21 °C, 21 °C, and 23 °C are the optimum phase change temperatures for 10 mm, 20 mm, 30 mm, and 40 mm PCM layer thicknesses, respectively. The highest energy saving amount is obtained as 188.0 kJ/m^2 for 20 mm PCM layer thickness and followed by 173.6 188.0 kJ/m^2 for 30 mm PCM layer thickness. The energy saving reaches only 84.2 kJ/m^2 and 120.7 kJ/m^2 for 10 mm and 40 mm PCM layer thicknesses, respectively. This indicates that an optimum PCM layer thickness occurs around the thickness of 20 mm, which will be discussed later. It is also important to note that the energy saving amounts for the PCM located near the outdoor are significantly lower than those of the PCM located near the indoor. However, contrary to the PCM located near inside, there is no zero values in the energy saving amounts in the case of PCM located near outside. This can be explained by the fact that the PCM layer is close to the exterior environment and is more susceptible to the changes in the outdoor climatic conditions, i.e., is easy to start phase change.

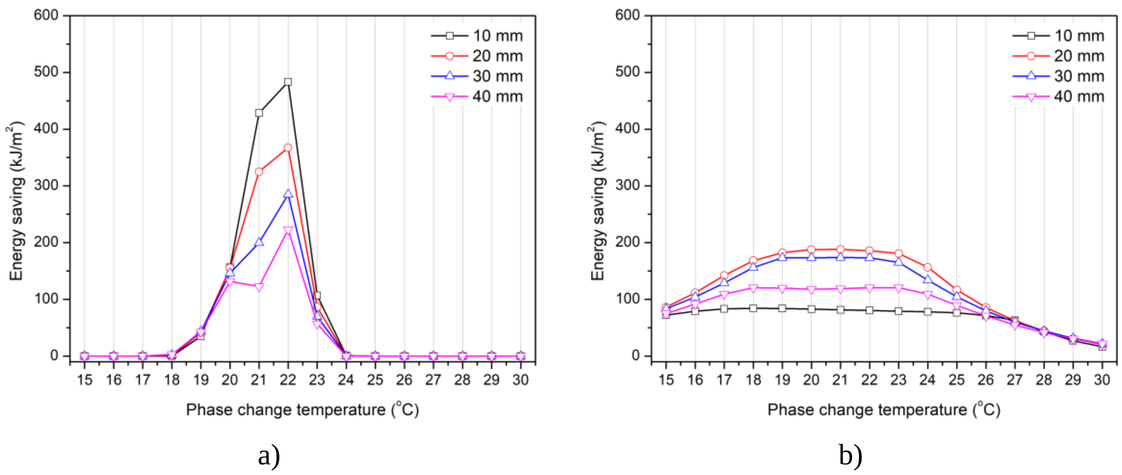

Figure 3.7. Energy saving amounts with respect to phase change temperature for selected PCM thicknesses (Method-3). a) PCM located near indoor (C1), b) PCM located near outdoor (C2)

Based on the maximum effect of latent heat utilization on the energy saving, the optimum melting temperature for each PCM layer thickness is found for both the inside and outside locations. The obtained values are given in Figure 3.8. It is noted that the optimum melting temperature for inside location is found as 22 °C regardless of the PCM layer thickness (the same as in Method-1). This finding indicates that the appropriate melting temperature of the PCM located near the outdoor is not affected by the PCM layer thickness. It should be pointed out that the indoor temperature is kept constant as 22 °C, so the optimum melting temperature is equal to the indoor temperature. However, the optimum melting temperature for the outside location significantly varies starting from 16 °C and reaches up to 23 °C depending on the PCM layer thickness. This phenomenon can be expected since the outside location is closer to the outdoor environment, and the PCM is more susceptible to the changes in the outdoor climatic conditions. An increasing trend for the optimum melting temperature can be clearly observed for the outside location as the thickness of the PCM layer is increased. Consequently, the optimum phase change temperature is constant and equal to the room temperature for the inside location regardless of the PCM layer thickness, and it varies significantly for the outside location depending on the layer thickness.

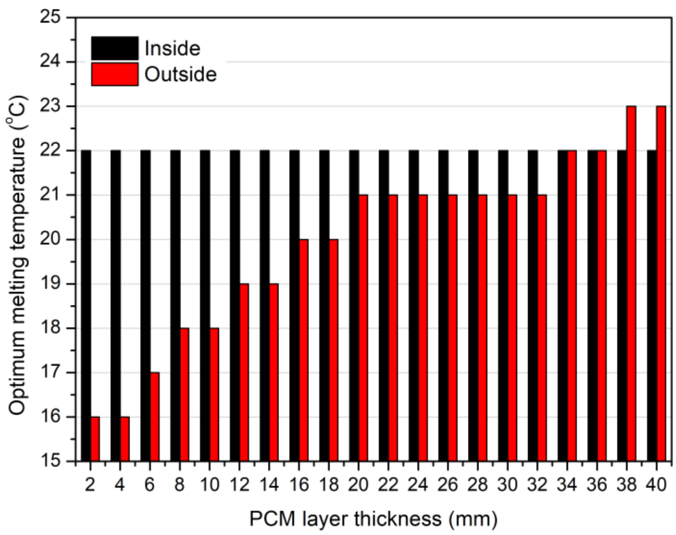

Figure 3.8. Optimum phase change temperature with respect to PCM layer thickness (Method-3)

In order to reveal if there is an optimum PCM layer thickness or not, energy saving amounts due to latent heat exploitation (E_{LH}) is calculated and given in Figure 3.9 with respect to each PCM layer thickness.

As can be clearly seen from the given figure, energy saving due to only latent heat activation behaves rather different for the inside and the outside locations. For the PCM located near the indoor, the energy saving amounts start from 186.5 kJ/m^2 (2 mm) reaches a peak point at 512.9 kJ/m^2 (8 mm) and then reduces to 223.2 kJ/m^2 (40 mm). The peak point, which is the highest energy saving value, is reached by 8 mm PCM layer thickness meaning that using higher or lower PCM layer thickness values degrade the energy saving potential of PCM. A similar behavior is also observed for the PCM located near the outdoor. However, it is noted that the energy saving amounts are significantly lower than those of PCM located near the indoor. For instance, energy saving amounts start from 13.6 kJ/m^2 (2 mm) reaches a peak point at 216.4 kJ/m^2 (24 mm) and then reduces to 120.7 kJ/m^2 (40 mm). An optimum value for the PCM layer thickness occurs as 24 mm which the PCM layer provides the highest energy saving amount when the PCM is located near the outdoor. There is a considerable amount of energy saving difference between the inside and outside location especially for the lower PCM layer thicknesses. For instance, only 13.6 kJ/m^2 energy saving is obtained for the outside location whereas this value radically jumps to 186.5 kJ/m^2 for the inside location, both for 2 mm PCM layer thickness. Apparently, this can be attributed to the latent heat impact of PCM on the energy saving performance. Besides, it is clear from the figure that locating the PCM layer near the indoor enables to save more energy than that of locating the PCM layer near the outdoor regardless of the PCM layer thickness.

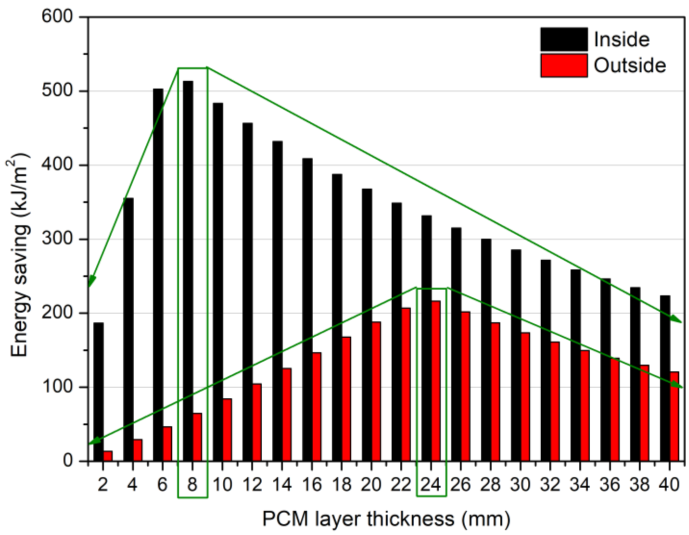

Figure 3.9. Energy saving amounts with respect to PCM layer thickness considering optimum melting temperature (Method-3)

This method shows that there an optimum melting temperature for the inside location (T_f = 22 °C) while the optimum melting temperature for the outside location significantly differs. Besides, it is observed that the energy saving due to latent heat activation is reached its maximum at certain PCM layer thicknesses for both locations meaning that there are optimum layer thicknesses.

3.1.4. Summary of the Optimized Parameters Based on Three Methods

Significant parameters, e.g., the melting temperature and layer thickness, affecting the PCM thermal performance is optimized considering three different methods in the previous sections. Here, optimal values for these parameters are given based on three methods for the sake of summarization of the findings. The obtained optimum melting temperatures (T_f) based on the three considered methods for the optimization case study are given in Figure 3.10. As can be seen for the indoor location of the PCM integration (Figure 3.10a), the optimum values for the melting temperature are the same for Method-1 and Method-3 (T_f = 22 °C). However, different optimum phase change temperatures are attained for Method-2 at certain layer thicknesses. For instance, T_f = 23 °C is found for 4 mm layer thickness while T_f = 21 °C is found for layer thicknesses between 16 mm and 34 mm. Considering the outdoor location for PCM integration, the optimum melting temperatures are observed to be fluctuates significantly between T_f = 16 °C and T_f = 26 °C depending on the PCM layer thickness (Figure 3.10b) as well as chosen method. It is interesting to note that the optimum melting temperatures are higher for Method-2 while they are lower for Method-1 and Method-3. The same T_f are determined for Method-1 and Method-3 similar to the inside location of the PCM integration although they differ depending on the layer thickness. The determined optimum PCM layer thicknesses for all of the considered methods and locations (near the indoor and outdoor) are given in Figure 3.11. As can be seen from the given figures, the optimum PCM layer thickness changes depending on the chosen method, i.e., optimization parameters, and the location of PCM.

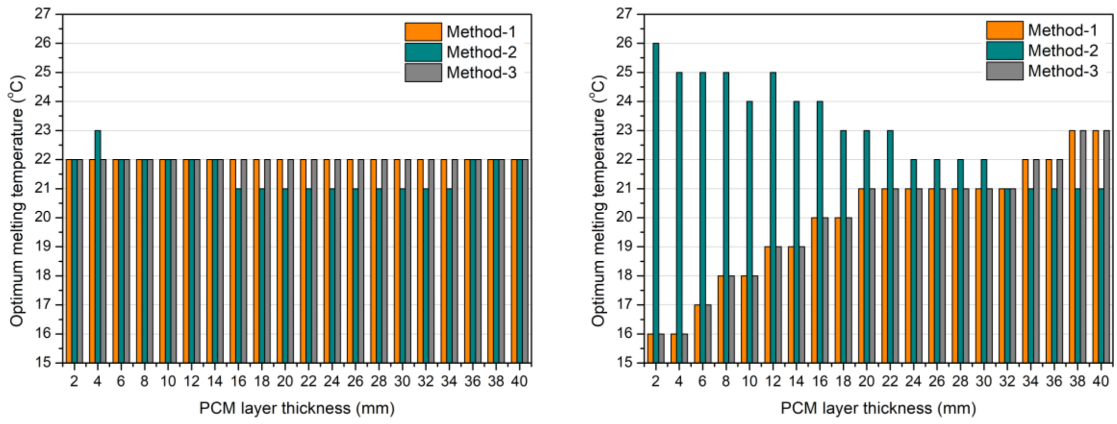

a) b)

Figure 3.10. Optimum melting temperatures (T_f) based on three methods for the indoor and outdoor locations, respectively. a) For the inside location (C1), b) For the outside location (C2)

However, it is noted that no optimum layer thickness is observed for Method-1 (based on E_{PCM}) considering both locations since higher the layer thickness of PCM, higher the energy saving. In Method-2 (based on MKR index), only the inside location of PCM gives an optimum PCM layer thickness, L_{PCM} = 34 mm, while no optimum layer thickness is attained for the outside location. Optimization based on E_{LH} (Method-3) provides optimum layer thicknesses for both locations on the other hand. The optimum PCM layer thicknesses are determined as 8 mm and 24 mm for the inside and outside locations, respectively.

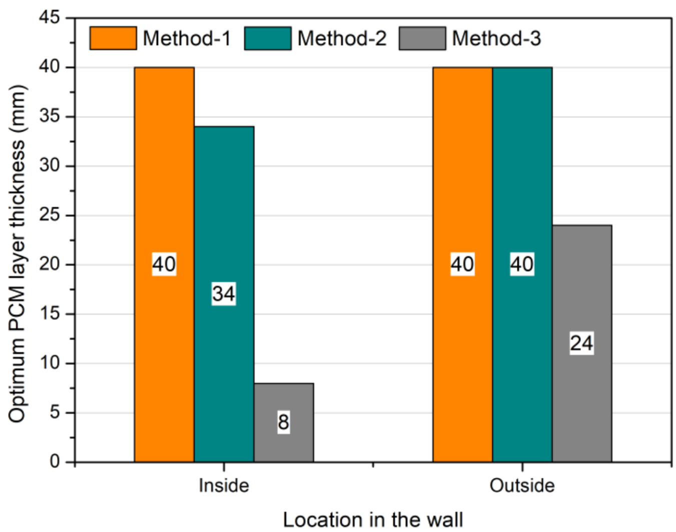

Figure 3.11. Optimum PCM layer thicknesses found based on three methods

It is obvious that analogy of PCM with insulation material is not fair since their thermophysical properties and application purposes are rather different from each other.

However, in building external wall applications, thermal performance of PCM and insulation material can be compared, and their interrelations can be revealed given that they both aim to reduce heat transfer between the indoor and outdoor. In this respect, parameters such as PCM melting temperature, location, and layer thickness need to be optimized in order to gain highest possible thermal performance from PCM so it can be evaluated together with insulation material. However, as demonstrated herein, each optimization approach can give a different optimum value which greatly affects the thermal performance of PCM application. Therefore, in the subsequent sections, Method-1 is chosen for optimization of PCM parameters since energy saving is the primary measure of insulation material utilization.

3.2. Thermal Performance of PCM Utilization Compared to Insulation

In this section, a comparison of PCM and insulation material (glass wool) is carried out to reveal the effect of PCM integration into building external wall in terms of energy saving performance. Although it is not fair head-to-head comparison of PCM and insulation material since their utilization purposes differ significantly, the obtained findings are given herein comparatively to assess how effective the PCM integration can be. In this respect, 20 different layer thicknesses (2 – 40 mm by 2 mm increment) for both PCM and insulation material are employed in two different locations, i.e., near the inside and near the outside. It should be noted that the PCM is used with its optimized melting temperatures which are given in the previous section. Besides, the optimized values based on Method-1 and Method-3 are used for melting temperature. The corresponding energy saving values for each of the considered layer thickness (for PCM and glass wool) are evaluated. The obtained energy saving values for both the glass wool and PCM for the inside location are given in Figure 3.12a. As expected, energy saving increases as the thickness of the layer is increased regardless of the used material (PCM or glass wool) since higher layer thickness provides greater thermal resistance and thermal mass inside the building external wall. The insulation material (glass wool) starts from 218.3 kJ/m^2 energy saving with 2 mm thickness and climbs at 931.5 kJ/m^2 energy saving with 40 mm thickness. It should be noted that the energy demand calculated for the reference wall (neither PCM nor glass wool containing case) is 1124.3 kJ/m^2. Based on that, it can be seen that a great amount of energy can be saved by only using insulation material in the wall. The corresponding energy demand reduction rates for 2 mm and 40 mm glass wool thicknesses are 19.4 % and 82.9 %. These are significant reductions in energy demand and show the importance of using insulation material. The PCM on the other hand saves 241.4 kJ/m^2 energy with 2 mm and 822.9 kJ/m^2 energy with 40 mm thickness. These energy saving values correspond to 21.5 % and 73.2 % reductions in energy demand compared to the reference case. It is not fair head-to-head comparison of an insulation material (glass wool in this case) and a PCM since their thermophysical properties and thus utilization purposes are rather different. For instance, the insulation material is used to strengthen thermal resistance due to its low thermal conductivity (k_{INS} = 0.038 W/(m.K)). On the other hand, the PCM is employed to increase thermal mass and store the thermal energy in the external wall due to its extremely high phase change enthalpy, i.e., latent heat (L_H = 134 kJ/m^2). However, although the fact that they cannot be compared head-to-head, the results are given comparatively herein to show how effective the PCM can be in energy saving despite its relatively high thermal conductivity (k_{PCM} = 0.20 W/(m.K)). It is surprising to find the PCM is more effective than the insulation material (glass wool) in energy saving performance for certain thicknesses, especially considering $k_{PCM} \approx 5.2 \times k_{INS}$. For instance, until the layer thickness 16 mm, the PCM is found to be saved more energy than the insulation material. However, after crossing the 16 mm turning point, the insulation material saved more energy than the PCM until to 40 mm thickness. The maximum difference in energy saving of the PCM (653.4 kJ/m^2) and the insulation material (472.9 kJ/m^2) is maximum at 6 mm with 180.5 kJ/m^2 value for the benefit of PCM. This is a great difference for 6 mm PCM thickness considering this difference corresponds to 16.1 % of the whole energy demand. It means that using 6 mm PCM with optimized melting temperature saves 58.1 % energy while using the same thickness glass wool saves only 42.1 % energy. On the other hand, the maximum difference in energy saving of the PCM (822.9 kJ/m^2) and the insulation material (931.5 kJ/m^2) is maximum at 40 mm with 108.6 kJ/m^2 value for the benefit of glass wool. Despite this value is still significant, the PCM is outperforms the insulation material in energy saving when used appropriately. These findings demonstrate that under a certain layer thickness (16 mm in this case) utilizing PCM instead of insulation material (glass wool) provides more energy saving. This outstanding performance of PCM over insulation material can be attributed to its high phase change enthalpy, i.e., great amount of thermal energy storage/release ability, despite its relatively high thermal conductivity. However, these observations are only valid for the inside location of PCM or insulation material, and the findings are rather different in the case of the outside location (Figure 3.12b). As can be clearly seen from the given figure, using the insulation material (glass wool) is always better than using the PCM for the outside location of the external wall. Energy saving with respect to reference case is calculated as 322.0 kJ/m^2 for 2 mm insulation thickness whereas 987.0 kJ/m^2 for 40 mm insulation thickness. Contrary to the inside location of PCM or insulation material, there is no turning point for the PCM layer thickness since the PCM is always saves less energy than the insulation material. The PCM energy saving amounts starts from 95.4 kJ/m^2 and climbs up to 822.7 kJ/m^2 with 2 mm and 40 mm, respectively. It is clear from the results that the insulation material (glass wool in this case) outperforms the PCM in all of the considered layer thicknesses for the outside location.

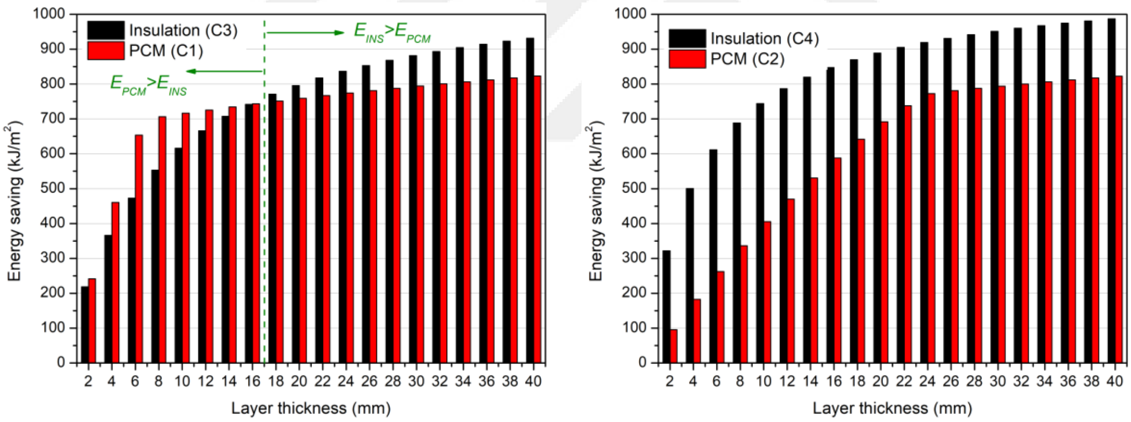

a) b)

Figure 3.12. Energy saving amount with respect to PCM and insulation layer thickness. a) For cases C1 and C3, b) For cases C2 and C4

This observation may seem controversial to the findings of the inside location. However, the optimum location of the insulation location is also dependent on the outdoor climatic conditions. Therefore, a comparison of the insulation material either locating it inside or outside position in the wall is performed to find the best location for the insulation material, i.e., glass wool, (Figure 3.13). According to the results obtained, locating insulating layer (glass wool) near the outside location performs better than that of near the inside location, regardless of the insulation layer thickness. For instance, energy demand is reduced by 70.8 % and 79.0 % for insulation positioned near the inside and outside, respectively, considering 20 mm layer thickness. Furthermore, energy demand reduction rate is reached up to 82.9 % and 87.8 % respectively for the inside and outside locations when 40 mm insulating layer is utilized. Therefore, it is clear that the optimized location of insulation material (glass wool) is near the outside location under the considered climatic conditions and for all of the thicknesses. In order to reveal the true energy saving potential of PCM integration, the energy saving amounts for the PCM and insulation material considering their best cases (inside and outside location, respectively) are given (Figure 3.14). As can be seen from the given figure, energy saving amount for insulation material is higher than that of PCM except for some layer thicknesses.

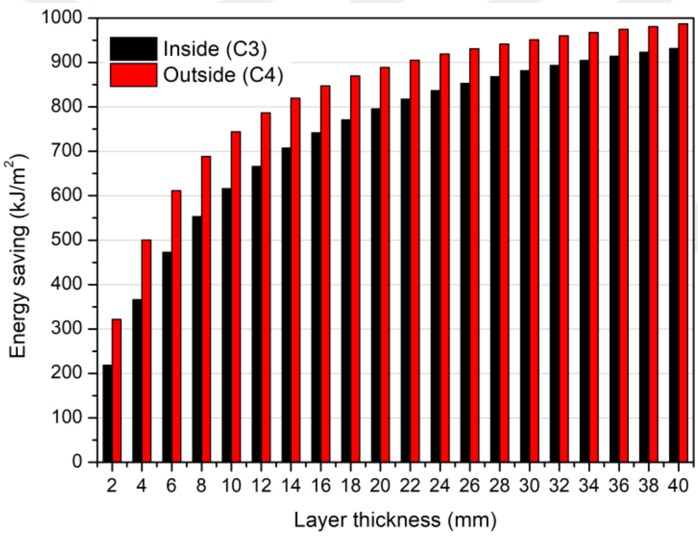

Figure 3.13. Energy saving amount with respect to insulation layer thickness for cases C3 and C4

It is interesting to note that utilizing PCM instead of insulation material (glass wool) is still able to provide higher energy saving considering 6 mm and 8 mm layer thicknesses. For instance, utilizing 6 mm PCM and 6 mm glass wool in the external wall delivers 653.43 kJ/m^2 and 611.67 kJ/m^2 energy saving amounts, respectively, meaning that utilizing 6 mm PCM instead of 6 mm glass wool provides 41.76 kJ/m^2 additional energy saving amount. Similarly, an additional energy saving amount of 18.17 kJ/m^2 is calculated in the case of using 8 mm PCM rather than 8 mm glass wool. It can be recalled that in the previous section the discussion related to latent heat contribution on energy saving (Method-3) it is stated that 6 mm and 8 mm PCM layer thicknesses provide the highest contribution of latent heat on energy saving. Therefore, the PCM being more effective than insulation material at 6 mm and 8 mm layer thicknesses can be explained due to the fact the latent heat exploitation is at maximum (based on Method-3) for these thicknesses. Consequently, the obtained results show that the PCM utilization can save as much or even more energy as insulation material under certain conditions, e.g., such as at specific layer thicknesses with optimum melting temperatures.

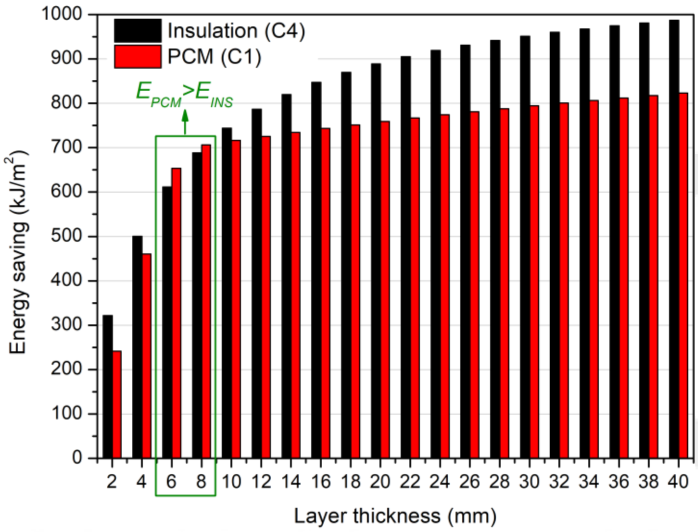

Figure 3.14. Energy saving amount with respect to PCM and insulation layer thickness for cases C1 and C4

3.3. Thermal Impact of Combination of PCM and Insulation on Energy Saving

In the previous section, the energy saving potential of PCM integration is found to be superior to that of insulation material under certain conditions. For instance, utilizing PCM is better than utilizing insulation material for 6 mm and 8 mm PCM layer thicknesses when outside location is chosen. Besides, under 16 mm layer thickness values for PCM and insulation material, the PCM outperforms the insulation material in terms of energy saving performance considering inside location. Therefore, an optimization study of layer thickness by using PCM and insulation combined is carried out considering different thickness ratio (ψ) values (Equation (2.1)). It is noted that ψ = 0 stands for L_{PCM} = 0 mm and L_{INS} = 40 mm, and ψ = 1 stands for L_{PCM} = 40 mm and L_{INS} = 0 mm. The optimization of PCM melting temperature is carried out for each considered case herein. Therefore, it should be noted that the energy saving results for

PCM corresponds to its optimized melting temperature for each PCM thickness ratio except for ψ = 0 which is fully insulation material. The optimum melting temperatures with respect to PCM thickness ratio are not given here but in the appendices for the sake of clarity of the discussion (APPENDIX A). In this context, different configurations of PCM and insulation integration is carried out and the obtained results are elaborated. The energy saving performance of inside location where PCM is closer to indoor location (C5) is given in Figure 3.15a. The red dashed line in the figure shows energy saving due to only insulation material (L_{INS} = 40 mm, ψ = 0) while the blue dashed line represents energy saving due to only PCM (L_{PCM} = 40 mm, ψ = 1). Besides, the dashed black line represents the energy saving due to PSM (no phase change) + insulation material combination. The PSM + insulation material results are given since the difference in energy saving values between PCM + insulation material and PSM + insulation material shows the energy saving due to latent heat activation (shown with orange arrow). As can be observed from the figure, the E_{LH} accounts a great deal of energy saving amount as expected. It is interesting to note that energy saving is significantly increased if the thickness ratio of PCM (ψ) is less than 0.6 (L_{PCM} = 24 mm and L_{INS} = 16 mm). Therefore, it can be suggested that $\psi < 0.6$ should be employed for building wall application of PCM and insulation for the highest possible energy saving performance considering inside location. However, it is crucial to state that ψ = 0 gives significantly less energy saving amount compared to $0 < \psi < 0.6$ conditions. The highest energy conservation is obtained with ψ = 0.05 (L_{PCM} = 2 mm and L_{INS} = 38 mm) meaning that an optimum value for PCM thickness ratio (ψ) occurs. The corresponding energy saving for ψ = 0.05 is calculated to be 999.4 kJ/m^2 while 931.5 kJ/m^2 is obtained in the case of ψ = 0. This finding shows that energy saving amount is increased by 7.3 % with respect to ψ = 0 (L_{INS} = 40 mm) if the optimum value of PCM thickness ratio is utilized (ψ = 0.05). It is also important to note that using only PCM in the wall is not adequate and gives the least energy saving amount (822.9 kJ/m^2) compared to using only insulation material as well as the combination of PCM and insulation material. Considering insulation material is closer to indoor for inside location (C6), the obtained energy saving amounts do not change for ψ = 0 and ψ = 1 cases (Figure 3.15b). However, they are observed to be varying significantly depending on the PCM thickness ratio (ψ). Similar to previous figure, energy saving amount is greatly increased for a certain ψ value which is found as ψ = 0.6. It is interesting to note that this value is the same critical value with that of in previous case (C5) meaning that sequence of PCM and insulation material does not affect that point for the inside location. The highest energy saving amount is obtained for ψ = 0.15 (L_{PCM} = 6 mm and L_{INS} = 32 mm) with value of 991.1 kJ/m^2 which corresponds to 6.4 % increase compared to using only insulation material (L_{INS} = 40 mm, ψ = 0). Consequently, the findings show that there is an optimum thickness ratio (ψ) for PCM and insulation material depending on the sequence of PCM and insulation material for the inside location.

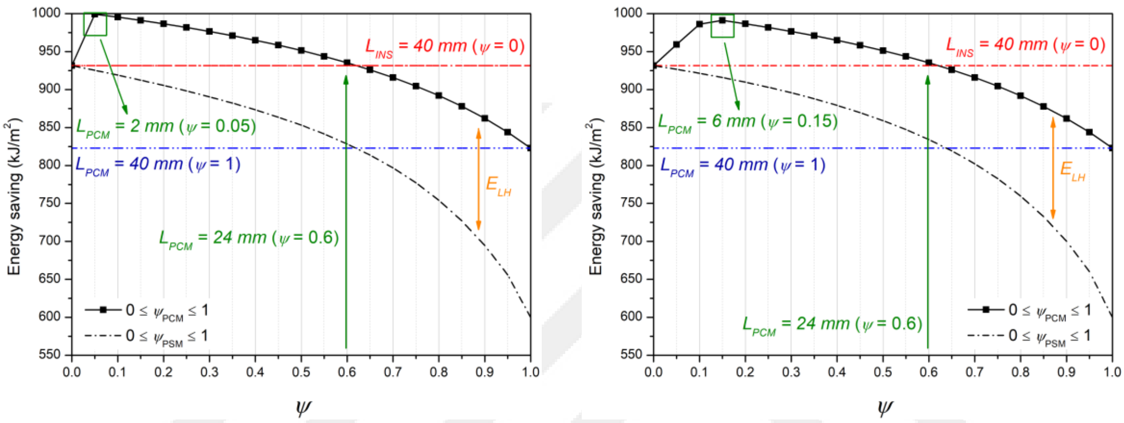

a) b)

Figure 3.15. Energy saving amount with respect to thickness ratio of PCM (ψ) for inside location and different sequences of PCM and insulation. a) For case C5, b) For case C6

The outside location is chosen for integration of PCM and insulation material, and the obtained findings are given in Figure 3.16. As can be seen from the given figure, the energy conservation amount is increased by using combination of PCM and insulation material instead of using only PCM or insulation material under certain conditions. The graph shows that 987 kJ/m^2 energy is saved by using only insulation material (ψ = 0) and 822.7 kJ/m^2 energy is saved by using only PCM (ψ = 1). The obtained results regarding the case of PCM is closer to outdoor (C7) are given in Figure 3.16a. The highest possible energy saving is calculated as 993.3 kJ/m^2 for utilizing a layer with PCM thickness ratio of ψ = 0.05 which corresponds to a marginal ~ 0.7 % increase in terms of energy saving compared to ψ = 0. On contrary to the findings presented so far in this section, utilizing combination of PCM and insulation material ($0 < \psi < 1$) does not enhance the energy saving amount compared to using only insulation material (ψ = 0) when insulation material is placed closer to outdoor (C8) (Figure 3.16b). This can be explained by the fact that locating insulating material near the outdoor reduces the heat transfer which in turn prevents phase change of PCM. Therefore, there is no critical value for ψ which gives a higher amount of energy saving than using only insulation material. As can be clearly observed from the given figure, the highest energy saving is attained by using only insulation material meaning that no PCM utilization is suggested for this configuration.

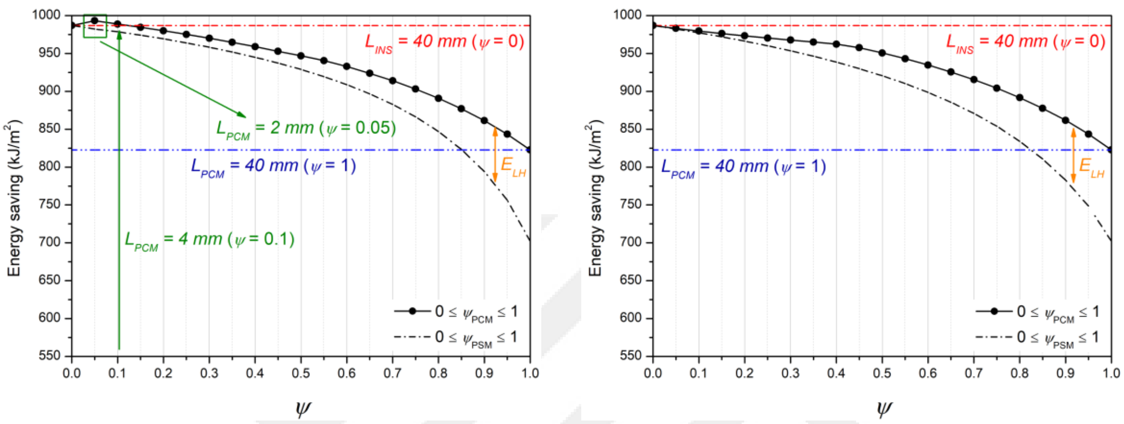

a) b)

Figure 3.16. Energy saving amount with respect to thickness ratio of PCM (ψ) for outside location and different sequences of PCM and insulation. a) For case C7, b) For case C8

In order to evaluate the thermal performance of PCM and insulation combination, energy saving with respect to different PCM thickness ratios ($0 \leq \psi \leq 1$) are obtained for PCM + insulation located near the indoor and outdoor separately. The thermal analyses are conducted, and the obtained findings are given in Figure 3.17. The results for PCM located near the indoor while insulation material located near the outdoor are given in Figure 3.17a. As can be seen from the given figure, combination of PCM and insulation material gives better thermal performance compared to only insulation material (ψ = 0) when ψ is lower than 0.15 and greater than 0. The highest energy saving amount (996.1 kJ/m^2) is obtained for thickness ratio of ψ = 0.05 (L_{PCM} = 2 mm and L_{INS} = 38 mm) suggesting utilization of 2 mm PCM and 38 mm insulation material at near the indoor and near the outdoor, respectively. The corresponding increase in energy saving amount is marginal and equals approximately ~ 1 % compared to only insulation material (ψ = 0). However, the situation is rather different for PCM located near the outdoor and insulation material located near the indoor case (Figure 3.17b). Energy saving performance of wall is considerably increased for $\psi \leq 0.6$ values meaning that the combination of PCM and insulation material outperforms using only insulation material in the wall. It is noted from the given figure that an optimum value for ψ occurs where energy saving is maximized. This value corresponds to ψ = 0.4 (L_{PCM} = 16 mm and L_{INS} = 24 mm) and the energy saving amount is calculated as 962.5 kJ/m^2 while using only insulation material provides 931.5 kJ/m^2. In this case, utilization of optimum thickness ratio of PCM (ψ = 0.4) in the wall enables 3.2 % increase in energy saving amount compared to only insulation material case (ψ = 0).

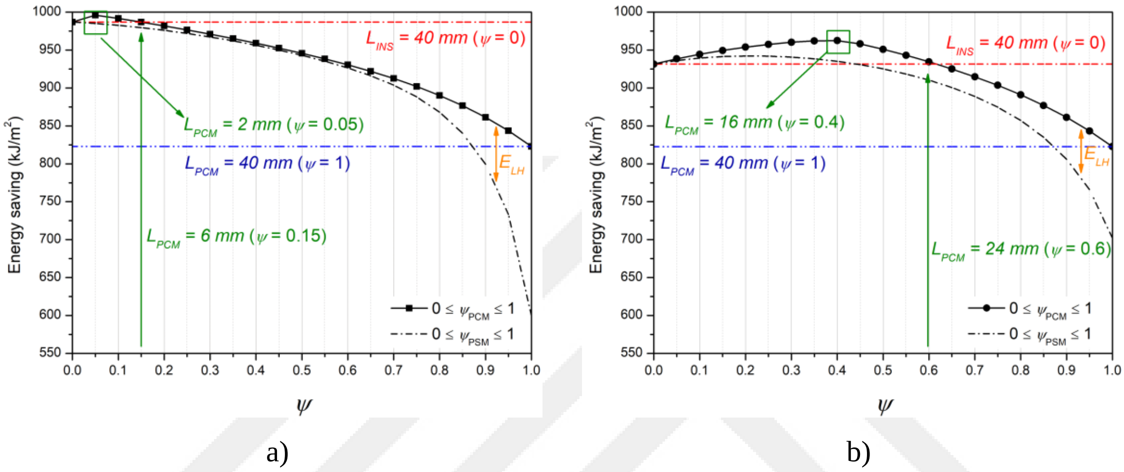

Figure 3.17. Energy saving amount with respect to thickness ratio of PCM (ψ) for outside and inside locations. a) For case C9, b) For case C10

3.4. A summary of the obtained results for all of the considered cases

Throughout the study, three different thermal performance evaluation methods for PCM are analyzed in order to optimize PCM melting temperature, thickness, and location in the wall. Then, energy saving performance of PCM is compared with that of the insulation wall at 20 different layer thicknesses. Furthermore, different combinations of PCM and insulation in the wall is investigated to reveal the case which provides the highest energy saving. Overall, 10 different wall configurations with PCM and insulation is studied and the optimum thickness (L_{PCM} and L_{INS}, if available), melting temperature ($T_{f,opt}$), and energy saving amounts are given in Table 3.1. It should be noted that the highest energy saving condition is given for each case, and the thickness and melting temperature corresponds to that condition. According to the obtained results, the highest possible energy saving is attained by using the PCM + insulation combination in the inside location and PCM is closer to indoor (C5) with ψ = 0.05. The determined energy saving is 999.4 kJ/m^2 and corresponds to an energy saving amount increase of 7.3 % compared to using only insulation material at the inside location (L_{INS} = 40 mm, ψ = 0). However, it is known that insulation performed better at the outside location (C4). The corresponding energy saving for 40 mm insulation material at the outside location (C4) is calculated as 987.0 kJ/m^2.Therefore, it can be fairly mentioned that utilizing C5 configuration with L_{PCM} = 2 mm and L_{INS} = 38 mm saves only 12.4 kJ/m^2 of energy compared to C4 (solely insulation) configuration. It is clear that this energy saving is marginal and insignificant since it only represents 1.3 % energy saving compared to insulation (C4). However, it should be recognized that this outcome is only valid for the considered problem and boundary conditions and needs further investigation with different climatic conditions. Despite that, these findings suggest that employing PCM and insulation material combination can provide more energy saving compared to insulation material in the wall.

Table 3.1. Summary of the results for all of the considered cases

Case	ψ	L_{PCM} **(mm)**	L_{INS} **(mm)**	$T_{f,opt}$ **(°C)**	**Energy saving (kJ/m²)**
C1	ψ = 1	40	−	22	822.9
C2	ψ = 1	40	−	23	822.7
C3	ψ = 0	−	40	−	931.5
C4	ψ = 0	−	40	−	987.0
C5	ψ = 0.05	2	38	22	999.4
C6	ψ = 0.15	6	34	22	991.1
C7	ψ = 0.05	2	38	22	993.3
C8	ψ = 0	0	40	−	987.0
C9	ψ = 0.05	2	38	22	996.1
C10	ψ = 0.40	16	24	20	962.5

4. CONCLUSION

In this study, the thermal performance of PCM integrated building external walls is evaluated based on three different methods/approaches. Therefore, an optimization case study of significant PCM parameters such as phase change temperature (T_f = 15 – 30 °C by 1 °C increment), PCM location (inside and outside), and PCM thickness (L_{PCM} = 2 – 40 mm by 2 mm increment) is performed. The obtained findings for these parameters are discussed to reveal their effect on the energy saving performance of PCM and their relation to chosen evaluation method. Furthermore, subsequent thermal analyses are performed to investigate the impact of PCM on the energy saving compared to insulation material. Although head-to-head comparison of PCM and insulation would not be fair since their utilization purposes are rather different, the obtained findings are still given comparatively to show the energy saving performance of PCM integration compared to insulation material. Thereafter, the thermal performance assessment of PCM and insulation material combination in the building external wall is conducted considering different PCM thickness ratios ($0 \leq \psi \leq 1$) while the total thickness of the wall is kept constant. In order to perform thermal analyses and obtain the necessary output parameters along with temperature field, an in-house code developed in Fortran programming language based on the finite difference approximation. The developed numerical code is then verified analytically and experimentally by Neumann's solution to phase change and an experimental work, respectively. The attained findings in this study can be summarized as follows:

- The optimum phase change temperature for the inside location is found as $T_{f,opt}$ = 22 °C regardless of PCM layer thickness based on M1 and M3. However, different optimum phase change temperatures (ranging between $T_{f,opt}$ = 21 °C and $T_{f,opt}$ = 23 °C) are observed depending on the PCM layer thickness considering M2.
- Considering the outdoor location for PCM integration, the optimum phase change temperatures ranges from $T_{f,opt}$ = 16 °C to $T_{f,opt}$ = 26 °C depending on the PCM layer thickness based on three methods. Despite that, M1 and M3 gives the same temperature values considering the same PCM layer thicknesses.
- The maximum energy saving is attained at 40 mm layer thickness for both inside and outside locations based on the analyses with M1 meaning that there is no

optimum value for PCM layer thickness. However, although no optimum thickness value is found for the inside location, $L_{PCM,opt}$ = 34 mm is observed for the inside location considering M2.

- Based on the thermal analyses with M3, it is revealed that $L_{PCM,opt}$ = 8 mm and $L_{PCM,opt}$ = 24 mm are the optimum thickness values for PCM integration.
- The comparative analyses of PCM and insulation material shows that energy saving performance of PCM can be better than insulation material considering the same location as well as the same thickness.
- It is observed that for the layer thicknesses below 16 mm, it is better to use PCM instead of insulation material considering the inside location. PCM integration with 6 mm saves 16.1 % more energy compared to the insulation material at the same thickness (and location).
- Considering both PCM (near the indoor, C1) and insulation material (near the outdoor, C4) at their optimum locations, PCM still provides more energy saving amount compared to insulation material for 6 mm and 8 mm layer thicknesses.
- Employing PCM and insulation material combination in the wall performs better than using only insulation material (at the same thickness) for certain configurations.
- Considering the case of C5, the highest possible energy saving is obtained by utilizing L_{PCM} = 2 mm and L_{INS} = 38 mm meaning that the optimum thickness ratio is ψ = 0.05. The corresponding energy saving for ψ = 0.05 (L_{PCM} = 2 mm and L_{INS} = 38 mm) is calculated to be 999.4 kJ/m^2 while 931.5 kJ/m^2 is obtained in the case of ψ = 0 (L_{INS} = 40 mm). This observation proves that energy saving of ψ = 0.05 is increased by 7.3 % compared to ψ = 0.
- A critical point for PCM thickness ratio, ψ, is observed for the cases C5, C6 and C10 meaning that the combination of PCM and insulation material outperforms the insulation material (ψ = 0) when $0 < \psi \leq 0.6$.
- Utilizing the combination of PCM and insulation material ($0 < \psi < 1$) does not enhance the energy saving compared to using only insulation material (ψ = 0) in the case of C8 meaning that employing insulation material always provides higher energy saving amount.

- The highest energy saving considering the combination of PCM and insulation material is attained with ψ = 0.05 (L_{PCM} = 2 mm and L_{INS} = 38 mm) in the configuration C5 by energy saving amount of 999.4 kJ/m^2. The highest energy for the insulation utilization on the other hand is obtained in the configuration C4 by energy saving amount of 987.0 kJ/m^2. Therefore, it can be mentioned that a marginal energy saving amount, around 12.5 kJ/m^2, is observed with C5 compared to C4.

It should be noted that the obtained findings are only valid for the considered problem and boundary conditions herein. According to the findings of the study, PCM outperforms insulation material at the same circumstances, and the combination of PCM + insulation material provides higher energy saving compared to solely insulation for some cases. However, since a hypothetical solar-air temperature profile is employed in this study to maximize the activation of latent heat of PCM, the thermal performance of PCM compared to insulation material can be poorer in practical applications. Besides, the combination of PCM and insulation material may not provide higher energy saving than insulation material considering the fact that a perfect daily melting-solidification cycle cannot always be ensured. In this respect, the thermal behavior of the considered wall configurations must be investigated under real climatic conditions in future work. Furthermore, different operating conditions for the considered building, e.g., intermittently or continuously heating/cooling of buildings, certainly affect the thermal behavior of the wall which can be also a future study topic.

REFERENCES

Abu-Hamdeh, N. H., Melaibari, A. A., Alquthami, T. S., Khoshaim, A., Oztop, H. F., & Karimipour, A. (2021). Efficacy of incorporating PCM into the building envelope on the energy saving and AHU power usage in winter. *Sustainable Energy Technologies and Assessments*, *43*, 100969. https://doi.org/10.1016/j.seta.2020.100969

Al-Saadi, S. N., & Zhai, Z. (John). (2015). Systematic evaluation of mathematical methods and numerical schemes for modeling PCM-enhanced building enclosure. *Energy and Buildings*, *92*, 374–388. https://doi.org/10.1016/j.enbuild.2015.01.044

AL-Saadi, S. N., & Zhai, Z. (John). (2013). Modeling phase change materials embedded in building enclosure: A review. *Renewable and Sustainable Energy Reviews*, *21*, 659–673. https://doi.org/10.1016/j.rser.2013.01.024

Arıcı, M., Bilgin, F., Nižetić, S., & Karabay, H. (2020). PCM integrated to external building walls: An optimization study on maximum activation of latent heat. *Applied Thermal Engineering*, *165*, 114560. https://doi.org/10.1016/j.applthermaleng.2019.114560

Arnault, A., Mathieu-Potvin, F., & Gosselin, L. (2010). Internal surfaces including phase change materials for passive optimal shift of solar heat gain. *International Journal of Thermal Sciences*, *49*(11), 2148–2156. https://doi.org/10.1016/j.ijthermalsci.2010.06.021

Asan, H., & Sancaktar, Y. S. (1998). Effects of Wall's thermophysical properties on time lag and decrement factor. *Energy and Buildings*, *28*(2), 159–166. https://doi.org/10.1016/S0378-7788(98)00007-3

Baetens, R., Jelle, B. P., & Gustavsen, A. (2010). Phase change materials for building applications: A state-of-the-art review. *Energy and Buildings*, *42*(9), 1361–1368. https://doi.org/10.1016/J.ENBUILD.2010.03.026

Ben Khedher, N., Bantan, R. A., Kolsi, L., & Omri, M. (2022). Performance investigation of a vertically configured LHTES via the combination of nano-enhanced PCM and fins: experimental and numerical approaches. *International Communications in Heat and Mass Transfer*, *137*, 106246. https://doi.org/10.1016/j.icheatmasstransfer.2022.106246

Bhamare, D. K., Rathod, M. K., & Banerjee, J. (2020). Numerical model for evaluating thermal performance of residential building roof integrated with inclined phase change material (PCM) layer. *Journal of Building Engineering*, *28*, 101018. https://doi.org/10.1016/J.JOBE.2019.101018

Bhamare, D. K., Rathod, M. K., & Banerjee, J. (2021). Proposal of a unique index for selection of optimum phase change material for effective thermal performance of a building envelope. *Solar Energy*, *218*, 129–141. https://doi.org/10.1016/j.solener.2021.02.027

Bolattürk, A. (2006). Determination of optimum insulation thickness for building walls with respect to various fuels and climate zones in Turkey. *Applied Thermal Engineering*, *26*(11–12), 1301–1309. https://doi.org/10.1016/j.applthermaleng.2005.10.019

Buratti, C., Belloni, E., Merli, F., & Zinzi, M. (2021). Aerogel glazing systems for building applications: A review. *Energy and Buildings*, *231*, 110587. https://doi.org/10.1016/J.ENBUILD.2020.110587

Cabeza, L. F., Castell, A., Barreneche, C., De Gracia, A., & Fernández, A. I. (2011). Materials used as PCM in thermal energy storage in buildings: A review. *Renewable and Sustainable Energy Reviews*, *15*(3), 1675–1695. https://doi.org/10.1016/J.RSER.2010.11.018

Cao, Y., Ayed, H., Algelany, A. M., Dahari, M., Phong Nguyen, P. Q., Gepreel, K. A., Nhanh Nguyen, V., Ehab, M., & Wae-Hayee, M. (2022). Receiving heat from a PCM tank by using natural convection of water and NEPCM: A simulation for LHTES application. *Case Studies in Thermal Engineering*, *35*, 102123. https://doi.org/10.1016/J.CSITE.2022.102123

Cesari, S., Emmi, G., & Bottarelli, M. (2022). A weather forecast-based control for the improvement of PCM enhanced radiant floors. *Applied Thermal Engineering*, *206*, 118119. https://doi.org/10.1016/J.APPLTHERMALENG.2022.118119

Çomakli, K., & Yüksel, B. (2003). Optimum insulation thickness of external walls for energy saving. *Applied Thermal Engineering*, *23*(4), 473–479. https://doi.org/10.1016/S1359-4311(02)00209-0

Çomakli, K., & Yüksel, B. (2004). Environmental impact of thermal insulation thickness in buildings. *Applied Thermal Engineering*, *24*(5–6), 933–940. https://doi.org/10.1016/J.APPLTHERMALENG.2003.10.020

Cuce, E., & Riffat, S. B. (2015). A state-of-the-art review on innovative glazing technologies. *Renewable and Sustainable Energy Reviews*, *41*, 695–714. https://doi.org/10.1016/J.RSER.2014.08.084

Dombayci, Ö. A. (2007). The environmental impact of optimum insulation thickness for external walls of buildings. *Building and Environment*, *42*(11), 3855–3859. https://doi.org/10.1016/J.BUILDENV.2006.10.054

Dombaycı, Ö. A., Gölcü, M., & Pancar, Y. (2006). Optimization of insulation thickness for external walls using different energy-sources. *Applied Energy*, *83*(9), 921–928. https://doi.org/10.1016/j.apenergy.2005.10.006

Fadl, M., & Eames, P. C. (2019). An experimental investigations of the melting of RT44HC inside a horizontal rectangular test cell subject to uniform wall heat flux. *International Journal of Heat and Mass Transfer*, *140*, 731–742. https://doi.org/10.1016/j.ijheatmasstransfer.2019.06.047

Global Alliance for Buildings and Construction, International Energy Agency, & The United Nations Environment Programme. (2020). *GlobalABC Roadmap for Buildings and Construction: Towards a zero-emission, efficient and resilient buildings and construction sector*. IEA Publications.

Hamidi, Y., Aketouane, Z., Malha, M., Bruneau, D., Bah, A., & Goiffon, R. (2021). Integrating PCM into hollow brick walls: Toward energy conservation in Mediterranean regions. *Energy and Buildings*, *248*, 111214. https://doi.org/10.1016/j.enbuild.2021.111214

Hassan, F., Jamil, F., Hussain, A., Ali, H. M., Janjua, M. M., Khushnood, S., Farhan, M., Altaf, K., Said, Z., & Li, C. (2022). Recent advancements in latent heat phase change materials and their applications for thermal energy storage and buildings: A state of the art review. *Sustainable Energy Technologies and Assessments*, *49*, 101646. https://doi.org/10.1016/J.SETA.2021.101646

Huang, H., Zhou, Y., Huang, R., Wu, H., Sun, Y., Huang, G., & Xu, T. (2020). Optimum insulation thicknesses and energy conservation of building thermal insulation materials in Chinese zone of humid subtropical climate. *Sustainable Cities and Society*, *52*, 101840. https://doi.org/10.1016/j.scs.2019.101840

International Energy Agency. (2021a). *Key World Energy Statistics 2021*. IEA Publications.

International Energy Agency. (2021b). *Net Zero by 2050: A Roadmap for the Global Energy Sector*. IEA Publications.

International Energy Agency. (2021c). *World Energy Outlook 2021*. IEA Publications.

Izquierdo-Barrientos, M. A., Belmonte, J. F., Rodríguez-Sánchez, D., Molina, A. E., & Almendros-Ibáñez, J. A. (2012). A numerical study of external building walls containing phase change materials (PCM). *Applied Thermal Engineering*, *47*, 73–85. https://doi.org/10.1016/j.applthermaleng.2012.02.038

Jiji, L. M. (2000). *Heat Conduction*. Springer.

Kalbasi, R., & Afrand, M. (2022). Which one is more effective to add to building envelope: Phase change material, thermal insulation, or their combination to meet zero-carbon-ready buildings? *Journal of Cleaner Production*, *367*, 133032. https://doi.org/10.1016/j.jclepro.2022.133032

Kaynakli, O. (2012). A review of the economical and optimum thermal insulation thickness for building applications. *Renewable and Sustainable Energy Reviews*, *16*(1), 415–425. https://doi.org/10.1016/J.RSER.2011.08.006

Kishore, R. A., Bianchi, M. V. A., Booten, C., Vidal, J., & Jackson, R. (2021). Parametric and sensitivity analysis of a PCM-integrated wall for optimal thermal load modulation in lightweight buildings. *Applied Thermal Engineering*, *187*, 116568. https://doi.org/10.1016/j.applthermaleng.2021.116568

Kouravand, A., Kasaeian, A., Pourfayaz, F., & Vaziri Rad, M. A. (2022). Evaluation of a nanofluid-based concentrating photovoltaic thermal system integrated with finned PCM heatsink: An experimental study. *Renewable Energy*, *201*, 1010–1025. https://doi.org/10.1016/J.RENENE.2022.11.025

Kuznik, F., David, D., Johannes, K., & Roux, J. J. (2011). A review on phase change materials integrated in building walls. *Renewable and Sustainable Energy Reviews*, *15*(1), 379–391. https://doi.org/10.1016/J.RSER.2010.08.019

Lamrani, B., Johannes, K., & Kuznik, F. (2021). Phase change materials integrated into building walls: An updated review. *Renewable and Sustainable Energy Reviews*, *140*, 110751. https://doi.org/10.1016/J.RSER.2021.110751

Li, C., Wen, X., Cai, W., Wu, J., Shao, J. J., Yang, Y., Yu, H., Liu, D., & Wang, M. (2022). Energy performance of buildings with composite phase-change material wallboards in different climatic zones of China. *Energy and Buildings*, *273*, 112398. https://doi.org/10.1016/J.ENBUILD.2022.112398

Li, D., Yang, R., Arıcı, M., Wang, B., Tunçbilek, E., Wu, Y., Liu, C., Ma, Z., & Ma, Y. (2022). Incorporating phase change materials into glazing units for building applications: Current progress and challenges. *Applied Thermal Engineering*, *210*, 118374. https://doi.org/10.1016/J.APPLTHERMALENG.2022.118374

Li, Q., Ju, Z., Wang, Z., Ma, L., Jiang, W., Li, D., & Jia, J. (2022). Thermal performance and economy of PCM foamed cement walls for buildings in different climate zones. *Energy and Buildings*, *277*, 112470. https://doi.org/10.1016/j.enbuild.2022.112470

Li, S., Zhu, N., Hu, P., Lei, F., & Deng, R. (2019). Numerical study on thermal performance of PCM Trombe Wall. *Energy Procedia*, *158*, 2441–2447. https://doi.org/10.1016/j.egypro.2019.01.317

Liu, S., Li, Y., & Zhang, Y. (2014). Mathematical solutions and numerical models employed for the investigations of PCMs′ phase transformations. *Renewable and Sustainable Energy Reviews*, *33*, 659–674. https://doi.org/10.1016/j.rser.2014.02.032

Long, L., & Ye, H. (2015). Effects of Thermophysical Properties of Wall Materials on Energy Performance in an Active Building. *Energy Procedia*, *75*, 1850–1855. https://doi.org/10.1016/J.EGYPRO.2015.07.161

Martin, K., Erkoreka, A., Flores, I., Odriozola, M., & Sala, J. M. (2011). Problems in the calculation of thermal bridges in dynamic conditions. *Energy and Buildings*, *43*(2–3), 529–535. https://doi.org/10.1016/J.ENBUILD.2010.10.018

Mazzeo, D., Oliveti, G., & Arcuri, N. (2017). Definition of a new set of parameters for the dynamic thermal characterization of PCM layers in the presence of one or more liquid-solid interfaces. *Energy and Buildings*, *141*, 379–396. https://doi.org/10.1016/j.enbuild.2017.02.027

Meng, E., Yu, H., & Zhou, B. (2017). Study of the thermal behavior of the composite phase change material (PCM) room in summer and winter. *Applied Thermal Engineering*, *126*, 212–225. https://doi.org/10.1016/j.applthermaleng.2017.07.110

Morrissey, J., Moore, T., & Horne, R. E. (2011). Affordable passive solar design in a temperate climate: An experiment in residential building orientation. *Renewable Energy*, *36*(2), 568–577. https://doi.org/10.1016/J.RENENE.2010.08.013

Ozel, M. (2011). Effect of wall orientation on the optimum insulation thickness by using a dynamic method. *Applied Energy*, *88*(7), 2429–2435. https://doi.org/10.1016/j.apenergy.2011.01.049

Özışık, M. N. (1980). *Heat Conduction*. Wiley.

Papadopoulos, A. M. (2005). State of the art in thermal insulation materials and aims for future developments. *Energy and Buildings*, *37*(1), 77–86. https://doi.org/10.1016/J.ENBUILD.2004.05.006

Salihi, M., El Fiti, M., Harmen, Y., Chhiti, Y., Chebak, A., M'Hamdi Alaoui, F. E., Achak, M., Bentiss, F., & Jama, C. (2022). Evaluation of global energy performance of building walls integrating PCM: Numerical study in semi-arid climate in Morocco. *Case Studies in Construction Materials*, *16*, e00979. https://doi.org/10.1016/j.cscm.2022.e00979

Souayfane, F., Biwole, P. H., Fardoun, F., & Achard, P. (2019). Energy performance and economic analysis of a TIM-PCM wall under different climates. *Energy*, *169*, 1274–1291. https://doi.org/10.1016/j.energy.2018.12.116

Sun, X., Zhang, Q., Medina, M. A., & Lee, K. O. (2014). Energy and economic analysis of a building enclosure outfitted with a phase change material board (PCMB). *Energy Conversion and Management*, *83*, 73–78. https://doi.org/10.1016/j.enconman.2014.03.035

Sun, X., Zhang, Y., Xie, K., & Medina, M. A. (2022). A parametric study on the thermal response of a building wall with a phase change material (PCM) layer for passive space cooling. *Journal of Energy Storage*, *47*, 103548. https://doi.org/10.1016/j.est.2021.103548

Theodosiou, T. G., & Papadopoulos, A. M. (2008). The impact of thermal bridges on the energy demand of buildings with double brick wall constructions. *Energy and Buildings, 40*(11), 2083–2089. https://doi.org/10.1016/J.ENBUILD.2008.06.006

Tunçbilek, E., Arıcı, M., Bouadila, S., & Wonorahardjo, S. (2020). Seasonal and annual performance analysis of PCM-integrated building brick under the climatic conditions of Marmara region. *Journal of Thermal Analysis and Calorimetry, 141*(1), 613–624. https://doi.org/10.1007/s10973-020-09320-8

Tunçbilek, E., Arıcı, M., Krajčík, M., Nižetić, S., & Karabay, H. (2020). Thermal performance based optimization of an office wall containing PCM under intermittent cooling operation. *Applied Thermal Engineering, 179,* 115750. https://doi.org/10.1016/j.applthermaleng.2020.115750

Tunçbilek, E., Komerska, A., & Arıcı, M. (2022). Optimisation of wall insulation thickness using energy management strategies: Intermittent versus continuous operation schedule. *Sustainable Energy Technologies and Assessments, 49,* 101778. https://doi.org/10.1016/j.seta.2021.101778

Turkish Standard: Thermal Insulation Requirements for Buildings (TS 825). (2013).

Uludaş, M. Ç., Tunçbilek, E., Yıldız, Ç., Arıcı, M., Li, D., & Krajčík, M. (2022). PCM-enhanced sunspace for energy efficiency and CO2 mitigation in a house in mediterranean climate. *Journal of Building Engineering, 57,* 104856. https://doi.org/10.1016/J.JOBE.2022.104856

United Nations Environment Programme. (2021). *2021 Global Status Report for Buildings and Construction: Towards a Zero-emission, Efficient and Resilient Buildings and Construction Sector*. UNEP Publications.

Wang, X., Yu, H., Li, L., & Zhao, M. (2016). Experimental assessment on the use of phase change materials (PCMs)-bricks in the exterior wall of a full-scale room. *Energy Conversion and Management, 120,* 81–89. https://doi.org/10.1016/j.enconman.2016.04.065

Ye, H., Long, L., Zhang, H., & Zou, R. (2014). The performance evaluation of shape-stabilized phase change materials in building applications using energy saving index. *Applied Energy, 113,* 1118–1126. https://doi.org/10.1016/j.apenergy.2013.08.067

Yu, J., Yang, C., Tian, L., & Liao, D. (2009). A study on optimum insulation thicknesses of external walls in hot summer and cold winter zone of China. *Applied Energy, 86*(11), 2520–2529. https://doi.org/10.1016/j.apenergy.2009.03.010

Zhang, S., Ma, Y., Li, D., Liu, C., & Yang, R. (2022). Thermal performance of a reversible multiple-glazing roof filled with two PCM. *Renewable Energy*, *182*, 1080–1093. https://doi.org/10.1016/J.RENENE.2021.11.008

Zhang, Y., Lin, K., Jiang, Y., & Zhou, G. (2008). Thermal storage and nonlinear heat-transfer characteristics of PCM wallboard. *Energy and Buildings*, *40*(9), 1771–1779. https://doi.org/10.1016/j.enbuild.2008.03.005

Zhou, G., Yang, Y., Wang, X., & Cheng, J. (2010). Thermal characteristics of shape-stabilized phase change material wallboard with periodical outside temperature waves. *Applied Energy*, *87*(8), 2666–2672. https://doi.org/10.1016/j.apenergy.2010.02.001

Zhou, G., Yang, Y., & Xu, H. (2011). Performance of shape-stabilized phase change material wallboard with periodical outside heat flux waves. *Applied Energy*, *88*(6), 2113–2121. https://doi.org/10.1016/j.apenergy.2011.01.016

Zhou, Z., Zhang, S., Wang, C., Zuo, J., He, Q., & Rameezdeen, R. (2016). Achieving energy efficient buildings via retrofitting of existing buildings: a case study. *Journal of Cleaner Production*, *112*, 3605–3615. https://doi.org/10.1016/J.JCLEPRO.2015.09.046

Zwanzig, S. D., Lian, Y., & Brehob, E. G. (2013). Numerical simulation of phase change material composite wallboard in a multi-layered building envelope. *Energy Conversion and Management*, *69*, 27–40. https://doi.org/10.1016/j.enconman.2013.02.003

APPENDICES

APPENDIX-A

The optimum melting temperatures for cases C5, C6, C7, C8, C9, and C10 with respect to PCM thickness ratio (ψ).

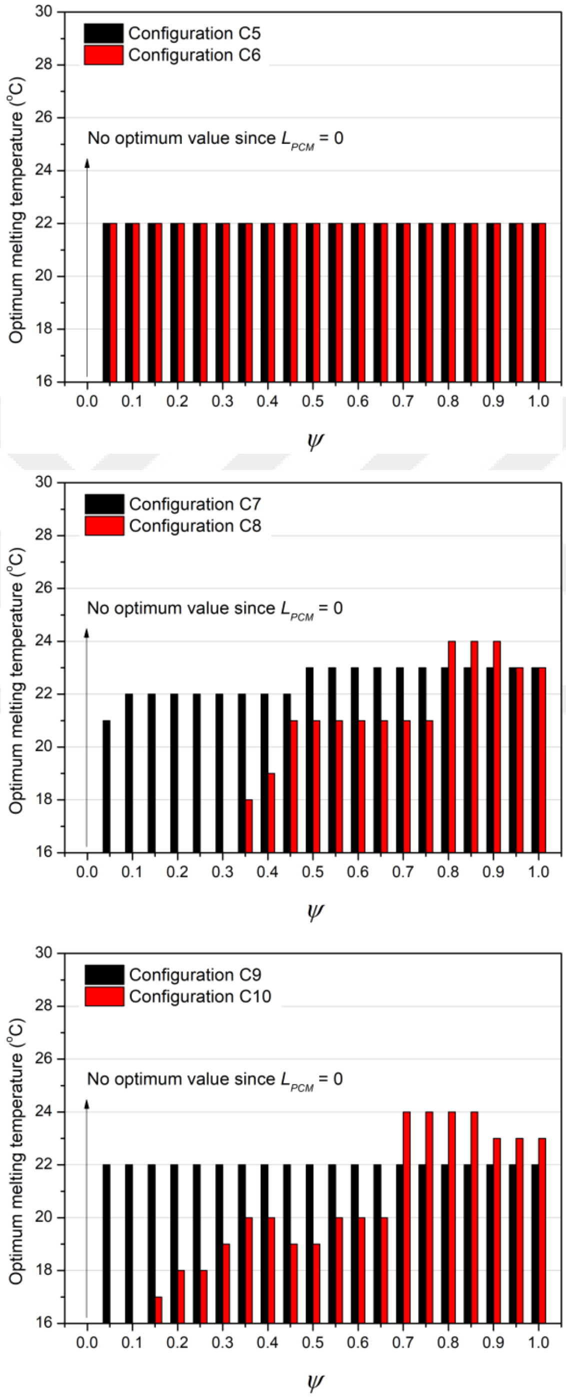

Figure A.1. The optimum melting temperatures with respect to PCM thickness ratios

PUBLICATIONS AND WORKS

Chati, D., Bouabdallah, S., Ghernaout, B., **Tunçbilek, E.**, Arıcı, M., & Driss, Z. (2021). Turbulent mixed convective heat transfer in a ventilated enclosure with a cylindrical/cubical heat source: a 3D analysis. *Energy Sources, Part A: Recovery, Utilization, and Environmental Effects*, 1–18. https://doi.org/10.1080/15567036.2021.1923872

Laouer, A., Teggar, M., **Tunçbilek, E.**, Arıcı, M., Hachani, L., & Ismail, K. A. R. (2022). Melting of hybrid nano-enhanced phase change material in an inclined finned rectangular cavity for cold energy storage. *Journal of Energy Storage*, *50*, 104185. https://doi.org/10.1016/j.est.2022.104185

Li, D., Yang, R., Arıcı, M., Wang, B., **Tunçbilek, E.**, Wu, Y., Liu, C., Ma, Z., & Ma, Y. (2022). Incorporating phase change materials into glazing units for building applications: Current progress and challenges. *Applied Thermal Engineering*, *210*, 118374. https://doi.org/10.1016/j.applthermaleng.2022.118374

Teggar, M., Arıcı, M., Mert, M. S., Mousavi Ajarostaghi, S. S., Niyas, H., **Tunçbilek, E.**, Ismail, K. A. R., Younsi, Z., Benhouia, A. T., & Mezaache, E. H. (2022). A comprehensive review of micro/nano enhanced phase change materials. *Journal of Thermal Analysis and Calorimetry*, *147*(6), 3989–4016. https://doi.org/10.1007/s10973-021-10808-0

Tükel, M., **Tunçbilek, E.**, Komerska, A., Keskin, G. A., & Arıcı, M. (2021). Reclassification of climatic zones for building thermal regulations based on thermoeconomic analysis: A case study of Turkey. *Energy and Buildings*, *246*, 111121. https://doi.org/10.1016/j.enbuild.2021.111121

Tunçbilek, E., Arıcı, M., Bouadila, S., & Wonorahardjo, S. (2020). Seasonal and annual performance analysis of PCM-integrated building brick under the climatic conditions of Marmara region. *Journal of Thermal Analysis and Calorimetry*, *141*(1), 613–624. https://doi.org/10.1007/s10973-020-09320-8

Tunçbilek, E., Arıcı, M., Krajčík, M., Li, Y., Jurčević, M., & Nižetić, S. (2022). Impact of nano-enhanced phase change material on thermal performance of building envelope and energy consumption. *International Journal of Energy Research*, *46*(14), 20249–20264. https://doi.org/10.1002/er.8200

Tunçbilek, E., Arıcı, M., Krajčík, M., Nižetić, S., & Karabay, H. (2020). Thermal performance based optimization of an office wall containing PCM under intermittent cooling operation. *Applied Thermal Engineering*, *179*, 115750. https://doi.org/10.1016/j.applthermaleng.2020.115750

Tunçbilek, E., Komerska, A., & Arıcı, M. (2022). Optimisation of wall insulation thickness using energy management strategies: Intermittent versus continuous operation schedule. *Sustainable Energy Technologies and Assessments*, *49*, 101778. https://doi.org/10.1016/j.seta.2021.101778

Uludas, M. C., Arici, M., **Tuncbilek, E.**, & Yildiz, C. (2021). On the sunspace utilization in a detached house in climatic conditions of Istanbul. *2021 6th International Conference on Smart and Sustainable Technologies (SpliTech)*, 1–6. https://doi.org/10.23919/SpliTech52315.2021.9566344

Uludaş, M. Ç., **Tunçbilek, E.**, Yıldız, Ç., Arıcı, M., Li, D., & Krajčík, M. (2022). PCM-enhanced sunspace for energy efficiency and CO2 mitigation in a house in mediterranean climate. *Journal of Building Engineering*, *57*, 104856. https://doi.org/10.1016/j.jobe.2022.104856

Wonorahardjo, S., Sutjahja, I. M., Mardiyati, Y., Andoni, H., Achsani, R. A., Steven, S., Thomas, D., **Tunçbilek, E.**, Arıcı, M., Rahmah, N., & Tedja, S. (2022). Effect of different building façade systems on thermal comfort and urban heat island phenomenon: An experimental analysis. *Building and Environment*, *217*, 109063. https://doi.org/10.1016/j.buildenv.2022.109063

Wonorahardjo, S., Sutjahja, I. M., **Tunçbilek, E.**, Achsani, R. A., Arıcı, M., & Rahmah, N. (2021). PCM-based passive air conditioner in urban houses for the tropical climates: An experimental analysis on the stratum air circulation. *Building and Environment*, *192*, 107632. https://doi.org/10.1016/j.buildenv.2021.107632

Wu, Y., Li, D., Jiang, W., Zhu, S., Zhao, X., Arıcı, M., & **Tunçbilek, E.** (2022). Energy storage and exergy efficiency analysis of a shell and tube latent thermal energy storage unit with non-uniform length and distributed fins. *Sustainable Energy Technologies and Assessments*, *53*, 102362. https://doi.org/10.1016/j.seta.2022.102362

BIOGRAPHY

Ekrem TUNÇBİLEK completed primary and high school in Aydın. He graduated in 2020 from Mechanical Engineering Department of Engineering Faculty at Kocaeli University. Following his graduation, he was accepted for MSc program at Department of Mechanical Engineering at Kocaeli University, Graduate School of Natural and Applied Sciences. Right after his acceptance for MSc program, he started to work as a research assistant in the same department in Thermodynamics and Heat Technique Division. He is still working as a research assistant and continuing research on subjects such as heat transfer, energy storage, phase change materials, thermal management, building energy saving, and computational fluid dynamics.